

Probe R -parity violating supersymmetry effects in $B \rightarrow K^{(*)}\ell^+\ell^-$ and $B_s \rightarrow \ell^+\ell^-$ decaysYuan-Guo Xu,¹ Ru-Min Wang,^{1,2} and Ya-Dong Yang^{1,*}¹*Department of Physics, Henan Normal University, XinXiang, Henan 453007, People's Republic of China*²*Institute of Particle Physics, Huazhong Normal University, Wuhan, Hubei 430070, People's Republic of China*

(Received 2 November 2006; published 21 December 2006)

We study the decays $B \rightarrow K^{(*)}\ell^+\ell^-$ and $B_s \rightarrow \ell^+\ell^-$ ($\ell = e, \mu$) in the minimal supersymmetric standard model with R -parity violation (RPV). From the recent measurements of $\mathcal{B}(B \rightarrow K^{(*)}\ell^+\ell^-)$ and the upper limits of $\mathcal{B}(B_s \rightarrow \ell^+\ell^-)$, we have derived new upper bounds on the relevant RPV coupling products, which are stronger than the existing ones. Using the constrained parameter space, we predict the RPV effects on the forward-backward asymmetries $\mathcal{A}_{\text{FB}}(B \rightarrow K^{(*)}\ell^+\ell^-)$ and the branching ratios $\mathcal{B}(B_s \rightarrow \ell^+\ell^-)$. Our results of the forward-backward asymmetries agree with the recent experiment data. It is also found that $\mathcal{B}(B_s \rightarrow \ell^+\ell^-)$ could be enhanced several orders by the RPV sneutrino exchange. The RPV effects on the dilepton invariant mass spectra of $B \rightarrow K^{(*)}\ell^+\ell^-$ and the normalized $\mathcal{A}_{\text{FB}}(B \rightarrow K^{(*)}\ell^+\ell^-)$ are studied in detail. Our results could be used to probe RPV effects and will correlate with searches for direct RPV signals at LHC.

DOI: [10.1103/PhysRevD.74.114019](https://doi.org/10.1103/PhysRevD.74.114019)

PACS numbers: 13.20.He, 11.30.Er, 12.15.Mm, 12.60.Jv

I. INTRODUCTION

Flavor changing neutral current (FCNC) $b \rightarrow s$ processes are forbidden at the tree level in the standard model (SM), which proceed at a low rate via penguin or box diagrams. If additional diagrams with non-SM particles contribute, their rates as well as other properties will be modified. This feature makes FCNC processes a powerful means to probe new physics indirectly. The recent experimental measurements of $B \rightarrow K^{(*)}\ell^+\ell^-$ decays [1–4] agree with the SM predictions within their error bars, therefore, these measurements will afford an opportunity to constrain new physics scenarios beyond the SM.

Semileptonic rare decays $B \rightarrow K^{(*)}\ell^+\ell^-$ have been extensively studied previously. The dominant perturbative SM contribution had been evaluated years ago [5], and later QCD corrections have been provided [6–8]. $\mathcal{O}(1/m_b^2)$ corrections have been first calculated in Ref. [9] and then in Refs. [10,11]. Long-distance contributions can have different origins according to the value of the dilepton invariant mass. The contributions of charmonium resonances to these decays by means of vector meson dominance (VMD) have been studied carefully [10,12–14]. Far from the resonance region, instead, $c\bar{c}$ long-distance effects are investigated using a heavy quark expansion in inverse powers of the charm-quark mass ($\mathcal{O}(1/m_c^2)$ corrections) [15]. Analyses of new physics contributions have been performed in different models, for example, the two-Higgs doublet model [16], the supersymmetric (SUSY) models [17,18], the SUSY SO(10) grand unification theory [19], and the top quark two-Higgs doublet model [20].

The effects of R -parity violation (RPV) SUSY in B meson decays have been extensively investigated in the literature [21,22]. The decays $B \rightarrow K^{(*)}\ell^+\ell^-$ and $B_s \rightarrow$

$\ell^+\ell^-$ are all induced at the parton level by the $b \rightarrow s\ell^+\ell^-$ process, and they involve the same set of the RPV coupling products. In this paper we will study the decays $B \rightarrow K^{(*)}\ell^+\ell^-$ and $B_s \rightarrow \ell^+\ell^-$ in the RPV SUSY model. Using the recent experimental data, we will obtain the new upper limits on the relevant RPV coupling products. Then we will use the constrained regions of the parameters to examine the RPV effects on the branching ratios of $B_s \rightarrow \ell^+\ell^-$ decays and the forward-backward asymmetries (\mathcal{A}_{FB}) of $B \rightarrow K^{(*)}\ell^+\ell^-$. In addition, we will compare the SM predictions with the RPV predictions about dilepton invariant mass spectra and the normalized forward-backward asymmetries in $B \rightarrow K^{(*)}\ell^+\ell^-$ decays.

The paper is arranged as follows. In Sec. II, we introduce the effective Hamiltonian and calculate the expressions for $B \rightarrow K^{(*)}\ell^+\ell^-$ and $B_s \rightarrow \ell^+\ell^-$ processes in the RPV SUSY. In Sec. III, we tabulate the theoretical inputs and deal with the numerical results. We display the constrained parameter spaces which satisfy all the available experimental data of $\mathcal{B}(B \rightarrow K^{(*)}\ell^+\ell^-)$ and the upper limits of $\mathcal{B}(B_s \rightarrow \ell^+\ell^-)$, and then we use the constrained parameter spaces to predict the RPV effects on $\mathcal{A}_{\text{FB}}(B \rightarrow K^{(*)}\ell^+\ell^-)$ and $\mathcal{B}(B_s \rightarrow \ell^+\ell^-)$, which have not been well measured yet. We also show the RPV effects on dilepton invariant mass spectra and the normalized forward-backward asymmetries in $B \rightarrow K^{(*)}\ell^+\ell^-$ decays. Section IV contains our summary and conclusion.

II. THE THEORETICAL FRAME FOR $B \rightarrow K^{(*)}\ell^+\ell^-$ AND $B_s \rightarrow \ell^+\ell^-$ **A. The decay branching ratios in the SM****1. The semileptonic decays $B \rightarrow K^{(*)}\ell^+\ell^-$**

In the SM, at the quark level, the rare semileptonic decays $b \rightarrow s\ell^+\ell^-$ can be described by the effective Hamiltonian

*Corresponding author
Electronic address: yangyd@henannu.edu.cn

$$\mathcal{H}_{\text{eff}}^{\text{SM}}(b \rightarrow s\ell^+\ell^-) = -\frac{G_F\alpha_e}{\sqrt{2}}V_{ts}^*V_{tb}\sum_{i=1}^{10}C_i(\mu)\mathcal{O}_i, \quad (1)$$

where the operator base \mathcal{O}_i is given in [7]. We will use the Wilson coefficients $C_i(\mu)$ calculated in the naive dimensional regularization (NDR) scheme [7], and the long-distance resonance effects on $C_9^{\text{eff}}(\mu)$ given in Refs. [12,14]. The Hamiltonian leads to the following free quark decay amplitude:

$$\begin{aligned} \mathcal{M}^{\text{SM}}(b \rightarrow s\ell^+\ell^-) &= \frac{G_F\alpha_e}{\sqrt{2}\pi}V_{ts}^*V_{tb}\left\{C_9^{\text{eff}}(\bar{s}\gamma_\mu P_L b)(\bar{\ell}\gamma^\mu\ell) \right. \\ &\quad + C_{10}(\bar{s}\gamma_\mu P_L b)(\bar{\ell}\gamma^\mu\gamma_5\ell) \\ &\quad \left. - 2\hat{m}_b C_7^{\text{eff}}\left(\bar{s}i\sigma_{\mu\nu}\frac{\hat{q}^\nu}{\hat{s}}P_R b\right)(\bar{\ell}\gamma^\mu\ell)\right\}, \end{aligned} \quad (2)$$

with $P_{L,R} \equiv (1 \mp \gamma_5)/2$, $s = q^2$ and $q = p_+ + p_-$ (p_\pm the four-momenta of the leptons). In our following calculations, we take $m_s/m_b = 0$, but keep the lepton masses. The hat denotes normalization in terms of the B -meson mass, m_B , e.g. $\hat{s} = s/m_B^2$, $\hat{m}_q = m_q/m_B$.

Exclusive decays $B \rightarrow K^{(*)}\ell^+\ell^-$ are described in terms of matrix elements of the quark operators in Eq. (2) over meson states, which can be parametrized by the form factors. It is worth noting the form factors involving the $B \rightarrow K^{(*)}$ transitions have been updated recently in [23].

Using Eq. (2), one can get the amplitudes of exclusive $B \rightarrow K^{(*)}\ell^+\ell^-$ decays

$$\begin{aligned} \mathcal{M}^{\text{SM}}(B \rightarrow K^{(*)}\ell^+\ell^-) &= \frac{G_F\alpha_e}{2\sqrt{2}\pi}V_{ts}^*V_{tb}m_B[\mathcal{T}_{1\mu}(\bar{\ell}\gamma^\mu\ell) \\ &\quad + \mathcal{T}_{2\mu}(\bar{\ell}\gamma^\mu\gamma_5\ell)], \end{aligned} \quad (3)$$

where for $B \rightarrow K\ell^+\ell^-$,

$$\mathcal{T}_{1\mu} = A'(\hat{s})\hat{p}_\mu + B'(\hat{s})\hat{q}_\mu, \quad (4)$$

$$\mathcal{T}_{2\mu} = C'(\hat{s})\hat{p}_\mu + D'(\hat{s})\hat{q}_\mu, \quad (5)$$

and for $B \rightarrow K^*\ell^+\ell^-$,

$$\begin{aligned} \mathcal{T}_{1\mu} &= A(\hat{s})\epsilon_{\mu\rho\alpha\beta}\epsilon^{*\rho}\hat{p}_B^\alpha\hat{p}_{K^*}^\beta - iB(\hat{s})\epsilon_\mu^* \\ &\quad + iC(\hat{s})(\epsilon^* \cdot \hat{p}_B)\hat{p}_\mu + iD(\hat{s})(\epsilon^* \cdot \hat{p}_B)\hat{q}_\mu, \end{aligned} \quad (6)$$

$$\begin{aligned} \mathcal{T}_{2\mu} &= E(\hat{s})\epsilon_{\mu\rho\alpha\beta}\epsilon^{*\rho}\hat{p}_B^\alpha\hat{p}_{K^*}^\beta - iF(\hat{s})\epsilon_\mu^* \\ &\quad + iG(\hat{s})(\epsilon^* \cdot \hat{p}_B)\hat{p}_\mu + iH(\hat{s})(\epsilon^* \cdot \hat{p}_B)\hat{q}_\mu, \end{aligned} \quad (7)$$

with $p = p_B + p_{K^{(*)}}$. Note that, using the equation of motion for lepton fields, the \hat{q}_μ terms in $\mathcal{T}_{1\mu}$ vanish, and those in $\mathcal{T}_{2\mu}$ become suppressed by one power of the lepton mass.

The auxiliary functions in $\mathcal{T}_{1\mu}$ and $\mathcal{T}_{2\mu}$ are defined as [18]

$$A'(\hat{s}) = C_9^{\text{eff}}(\hat{s})f_+(\hat{s}) + \frac{2\hat{m}_b}{1 + \hat{m}_K}C_7^{\text{eff}}f_T(\hat{s}), \quad (8)$$

$$B'(\hat{s}) = C_9^{\text{eff}}(\hat{s})f_-(\hat{s}) - \frac{2\hat{m}_b}{\hat{s}}(1 - \hat{m}_K)C_7^{\text{eff}}f_T(\hat{s}), \quad (9)$$

$$C'(\hat{s}) = C_{10}f_+(\hat{s}), \quad (10)$$

$$D'(\hat{s}) = C_{10}f_-(\hat{s}), \quad (11)$$

$$A(\hat{s}) = \frac{2}{1 + \hat{m}_{K^*}}C_9^{\text{eff}}(\hat{s})V(\hat{s}) + \frac{4\hat{m}_b}{\hat{s}}C_7^{\text{eff}}T_1(\hat{s}), \quad (12)$$

$$\begin{aligned} B(\hat{s}) &= (1 + \hat{m}_{K^*})\left[C_9^{\text{eff}}(\hat{s})A_1(\hat{s}) \right. \\ &\quad \left. + \frac{2\hat{m}_b}{\hat{s}}(1 - \hat{m}_{K^*})C_7^{\text{eff}}T_2(\hat{s})\right], \end{aligned} \quad (13)$$

$$\begin{aligned} C(\hat{s}) &= \frac{1}{1 - \hat{m}_{K^*}^2}\left[(1 - \hat{m}_{K^*})C_9^{\text{eff}}(\hat{s})A_2(\hat{s}) \right. \\ &\quad \left. + 2\hat{m}_b C_7^{\text{eff}}\left(T_3(\hat{s}) + \frac{1 - \hat{m}_{K^*}}{\hat{s}}T_2(\hat{s})\right)\right], \end{aligned} \quad (14)$$

$$\begin{aligned} D(\hat{s}) &= \frac{1}{\hat{s}}\left[C_9^{\text{eff}}(\hat{s})((1 + \hat{m}_{K^*})A_1(\hat{s}) - (1 - \hat{m}_{K^*})A_2(\hat{s})) \right. \\ &\quad \left. - 2\hat{m}_{K^*}A_0(\hat{s}) - 2\hat{m}_b C_7^{\text{eff}}T_3(\hat{s})\right], \end{aligned} \quad (15)$$

$$E(\hat{s}) = \frac{2}{1 + \hat{m}_{K^*}}C_{10}V(\hat{s}), \quad (16)$$

$$F(\hat{s}) = (1 + \hat{m}_{K^*})C_{10}A_1(\hat{s}), \quad (17)$$

$$G(\hat{s}) = \frac{1}{1 + \hat{m}_{K^*}}C_{10}A_2(\hat{s}), \quad (18)$$

$$\begin{aligned} H(\hat{s}) &= \frac{1}{\hat{s}}C_{10}\left[(1 + \hat{m}_{K^*})A_1(\hat{s}) - (1 - \hat{m}_{K^*})A_2(\hat{s}) \right. \\ &\quad \left. - 2\hat{m}_{K^*}A_0(\hat{s})\right]. \end{aligned} \quad (19)$$

It is noted that the inclusion of the full s -quark mass dependence in the above formulae can be done by substituting $m_b \rightarrow m_b + m_s$ into all terms proportional to $C_7^{\text{eff}}T_1$ and $C_7^{\text{eff}}f_T$ and $m_b \rightarrow m_b - m_s$ in $C_7^{\text{eff}}T_{2,3}$, since $\mathcal{O}_7 \sim \bar{s}\sigma_{\mu\nu}[(m_b + m_s) + (m_b - m_s)\gamma_5]q^\nu b$.

The kinematic variables (\hat{s}, \hat{u}) are chosen to be

$$\hat{s} = \hat{q}^2 = (\hat{p}_+ + \hat{p}_-)^2, \quad (20)$$

$$\hat{u} = (\hat{p}_B - \hat{p}_-)^2 - (\hat{p}_B - \hat{p}_+)^2, \quad (21)$$

which are bounded as

$$(2\hat{m}_\ell)^2 \leq \hat{s} \leq (1 - \hat{m}_{K^{(*)}})^2, \quad (22)$$

$$-\hat{u}(\hat{s}) \leq \hat{u} \leq \hat{u}(\hat{s}), \quad (23)$$

with $\hat{m}_\ell = m_\ell/m_B$ and

$$\hat{u}(\hat{s}) = \sqrt{\lambda \left(1 - 4 \frac{\hat{m}_\ell^2}{\hat{s}}\right)}, \quad (24)$$

$$\lambda \equiv \lambda(1, \hat{m}_{K^{(*)}}^2, \hat{s}) = 1 + \hat{m}_{K^{(*)}}^4 + \hat{s}^2 - 2\hat{s} - 2\hat{m}_{K^{(*)}}^2(1 + \hat{s}). \quad (25)$$

The variable \hat{u} corresponds to θ , the angle between the momentum of the B -meson and the lepton ℓ^+ in the

dilepton center-of-mass system (CMS) frame, through the relation $\hat{u} = -\hat{u}(s) \cos\theta$ [14]. Keeping the lepton mass, we find the double differential decay branching ratios \mathcal{B}^K and \mathcal{B}^{K^*} for the decays $B \rightarrow K \ell^+ \ell^-$ and $B \rightarrow K^* \ell^+ \ell^-$, respectively, as

$$\begin{aligned} \frac{d^2 \mathcal{B}_{\text{SM}}^K}{d\hat{s}d\hat{u}} &= \tau_B \frac{G_F^2 \alpha_e^2 m_B^5}{2^{11} \pi^5} |V_{ts}^* V_{tb}|^2 \{ (|A'|^2 + |C'|^2)(\lambda - \hat{u}^2) \\ &\quad + |C'|^2 4\hat{m}_\ell^2 (2 + 2\hat{m}_K^2 - \hat{s}) + \text{Re}(C'D'^*) \\ &\quad \times 8\hat{m}_\ell^2 (1 - \hat{m}_K^2) + |D'|^2 4\hat{m}_\ell^2 \hat{s} \}, \end{aligned} \quad (26)$$

$$\begin{aligned} \frac{d^2 \mathcal{B}_{\text{SM}}^{K^*}}{d\hat{s}d\hat{u}} &= \tau_B \frac{G_F^2 \alpha_e^2 m_B^5}{2^{11} \pi^5} |V_{ts}^* V_{tb}|^2 \left\{ \frac{|A|^2}{4} (\hat{s}(\lambda + \hat{u}^2) + 4\hat{m}_\ell^2 \lambda) + \frac{|E|^2}{4} (\hat{s}(\lambda + \hat{u}^2) - 4\hat{m}_\ell^2 \lambda) \right. \\ &\quad + \frac{1}{4\hat{m}_{K^*}^2} [|B|^2 (\lambda - \hat{u}^2 + 8\hat{m}_{K^*}^2 (\hat{s} + 2\hat{m}_\ell^2)) + |F|^2 (\lambda - \hat{u}^2 + 8\hat{m}_{K^*}^2 (\hat{s} - 4\hat{m}_\ell^2))] - 2\hat{s} \hat{u} [\text{Re}(BE^*) + \text{Re}(AF^*)] \\ &\quad + \frac{\lambda}{4\hat{m}_{K^*}^2} [|C|^2 (\lambda - \hat{u}^2) + |G|^2 (\lambda - \hat{u}^2 + 4\hat{m}_\ell^2 (2 + 2\hat{m}_{K^*}^2 - \hat{s}))] - \frac{1}{2\hat{m}_{K^*}^2} [\text{Re}(BC^*) (1 - \hat{m}_{K^*}^2 - \hat{s}) (\lambda - \hat{u}^2) \\ &\quad \left. + \text{Re}(FG^*) ((1 - \hat{m}_{K^*}^2 - \hat{s}) (\lambda - \hat{u}^2) + 4\hat{m}_\ell^2 \lambda) \right] - 2 \frac{\hat{m}_\ell^2}{\hat{m}_{K^*}^2} \lambda [\text{Re}(FH^*) - \text{Re}(GH^*) (1 - \hat{m}_{K^*}^2)] + |H|^2 \frac{\hat{m}_\ell^2}{\hat{m}_{K^*}^2} \hat{s} \lambda \}. \end{aligned} \quad (27)$$

Our results of the double differential decay branching ratios are consistent with the ones in Ref. [18].

2. The pure leptonic decays $B_s \rightarrow \ell^+ \ell^-$

In the SM, the effective Hamiltonian has been given by [24]

$$\begin{aligned} \mathcal{H}_{\text{eff}}^{\text{SM}}(B_s \rightarrow \ell^+ \ell^-) &= -\frac{G_F}{\sqrt{2}} \frac{\alpha_e}{2\pi \sin^2 \theta_W} V_{ts}^* V_{tb} \\ &\quad \times Y(x_t) (\bar{s}b)_{V-A} (\bar{\ell}\ell)_{V-A} + \text{H.c.}, \end{aligned} \quad (28)$$

where $x_t = \frac{m_t^2}{m_W^2}$, $m_t \equiv \bar{m}_t(m_t)$, $(\bar{s}b)_{V-A} \equiv \bar{s} \gamma_\mu (1 - \gamma_5) b$.

The pure leptonic decay amplitudes can be written as

$$\mathcal{M}^{\text{SM}}(B_s \rightarrow \ell^+ \ell^-) = h_{\text{SM}} (\bar{\ell} \not{p}_B (1 - \gamma_5) \ell), \quad (29)$$

with

$$h_{\text{SM}} = -\frac{G_F}{\sqrt{2}} \frac{\alpha_e}{2\pi \sin^2 \theta_W} V_{ts}^* V_{tb} Y(x_t) (i f_{B_s}). \quad (30)$$

Then we can get the branching ratios for $B_s \rightarrow \ell^+ \ell^-$

$$\begin{aligned} \mathcal{B}^{\text{SM}}(B_s \rightarrow \ell^+ \ell^-) &= \frac{\tau_{B_s}}{16\pi m_{B_s}} \sqrt{1 - 4\hat{m}_\ell^2} |\mathcal{M}^{\text{SM}}(B_s \rightarrow \ell^+ \ell^-)|^2 \\ &= \tau_{B_s} \frac{G_F^2}{\pi} \left(\frac{\alpha_e}{4\pi \sin^2 \theta_W} \right)^2 f_{B_s}^2 m_\ell^2 m_{B_s} \\ &\quad \times \sqrt{1 - 4\hat{m}_\ell^2} |V_{ts}^* V_{tb}|^2 Y^2(x_t). \end{aligned} \quad (31)$$

B. The decay amplitudes in RPV SUSY

In the most general superpotential of the minimal supersymmetric standard model (MSSM), the RPV superpotential is given by [25]

$$\begin{aligned} \mathcal{W}_{\mathcal{R}_p} &= \mu_i \hat{L}_i \hat{H}_u + \frac{1}{2} \lambda_{[ijk]} \hat{L}_i \hat{L}_j \hat{E}_k^c + \lambda'_{ijk} \hat{L}_i \hat{Q}_j \hat{D}_k^c \\ &\quad + \frac{1}{2} \lambda''_{[ijk]} \hat{U}_i^c \hat{D}_j^c \hat{D}_k^c, \end{aligned} \quad (32)$$

where \hat{L} and \hat{Q} are the SU(2) doublet lepton and quark superfields, respectively. \hat{E}^c , \hat{U}^c , and \hat{D}^c are the singlet superfields, while i , j , and k are generation indices and c denotes a charge conjugate field.

The bilinear RPV superpotential terms $\mu_i \hat{L}_i \hat{H}_u$ can be rotated away by suitable redefining of the lepton and Higgs superfields [26]. However, the rotation will generate a soft SUSY breaking bilinear term which would affect our calculation through loop level. However, the processes discussed in this paper could be induced by tree-level RPV couplings, so that we would neglect subleading RPV loop contributions in this study.

The λ and λ' couplings in Eq. (32) break the lepton number, while the λ'' couplings break the baryon number. There are 27 λ'_{ijk} couplings, 9 λ_{ijk} and 9 λ''_{ijk} couplings. $\lambda_{[ijk]}$ are antisymmetric with respect to their first two indices, and $\lambda''_{[ijk]}$ are antisymmetric with j and k .

From Eq. (32), we can obtain the relevant four fermion effective Hamiltonian for the $b \rightarrow s \ell \ell$ process due to the squarks and sneutrinos exchanges

$$\begin{aligned} \mathcal{H}_{\text{eff}}^{\mathcal{R}_p} = & \frac{1}{2} \sum_i \frac{\lambda'_{jik} \lambda_{lin}^{I*}}{m_{\tilde{u}_{iL}}^2} (\bar{d}_k \gamma^\mu P_R d_n) (\bar{\ell}_l \gamma_\mu P_L \ell_j) \\ & + \frac{1}{2} \sum_i \left\{ \frac{\lambda_{ijk} \lambda_{imn}^{I*}}{m_{\tilde{\nu}_{iL}}^2} (\bar{d}_m P_R d_n) (\bar{\ell}_k P_L \ell_j) \right. \\ & \left. + \frac{\lambda_{ijk}^* \lambda_{imn}^{I'}}{m_{\tilde{\nu}_{iL}}^2} (\bar{d}_n P_L d_m) (\bar{\ell}_j P_R \ell_k) \right\}. \end{aligned} \quad (33)$$

The RPV feynman diagrams for $B \rightarrow K^{(*)} \ell^+ \ell^-$ and $B_s \rightarrow \ell^+ \ell^-$ are displayed in Figs. 1 and 2, respectively.

From Eq. (33), we can obtain the RPV decay amplitude for $B \rightarrow K \ell^+ \ell^-$

$$\begin{aligned} \mathcal{M}^{\mathcal{R}_p}(B \rightarrow K \ell^+ \ell^-) = & \Delta_{\tilde{u}} (\bar{\ell}_k (\not{p}_B + \not{p}_K) (1 - \gamma_5) \ell_j) \\ & + \Delta_{\tilde{\nu}} (\bar{\ell}_k (1 - \gamma_5) \ell_j) \\ & + \Delta'_{\tilde{\nu}} (\bar{\ell}_k (1 + \gamma_5) \ell_j), \end{aligned} \quad (34)$$

with

$$\Delta_{\tilde{u}} = \sum_i \frac{\lambda'_{ji3} \lambda_{ki2}^{I*}}{8m_{\tilde{u}_{iL}}^2} f_+^{B \rightarrow K}(\hat{s}), \quad (35)$$

$$\Delta_{\tilde{\nu}} = \sum_i \frac{\lambda_{ijk} \lambda_{i32}^{I*}}{8m_{\tilde{\nu}_{iL}}^2} f_+^{B \rightarrow K}(\hat{s}) \frac{m_B^2 - m_K^2}{\bar{m}_b - \bar{m}_s}, \quad (36)$$

$$\Delta'_{\tilde{\nu}} = \sum_i \frac{\lambda_{ikj}^* \lambda'_{i23}}{8m_{\tilde{\nu}_{iL}}^2} f_+^{B \rightarrow K}(\hat{s}) \frac{m_B^2 - m_K^2}{\bar{m}_b - \bar{m}_s}, \quad (37)$$

and \bar{m}_b and \bar{m}_s the quark's running masses at the scale m_b .

For $B \rightarrow K^* \ell^+ \ell^-$, the RPV amplitude is

$$\begin{aligned} \mathcal{M}^{\mathcal{R}_p}(B \rightarrow K^* \ell^+ \ell^-) = & \mathcal{T}_{3\mu} (\bar{\ell}_k \gamma^\mu (1 - \gamma_5) \ell_j) \\ & + \Omega_{\tilde{\nu}} (\bar{\ell}_k (1 - \gamma_5) \ell_j) \\ & + \Omega'_{\tilde{\nu}} (\bar{\ell}_k (1 + \gamma_5) \ell_j), \end{aligned} \quad (38)$$

where

$$\begin{aligned} \mathcal{T}_{3\mu} = & I(\hat{s}) \epsilon_{\mu\rho\alpha\beta} \epsilon^{*\rho} \hat{p}_B^\alpha \hat{p}_{K^*}^\beta - iJ(\hat{s}) \epsilon_\mu^* + iK(\hat{s}) (\epsilon^* \cdot \hat{p}_B) \hat{p}_\mu \\ & + iL(\hat{s}) (\epsilon^* \cdot \hat{p}_B) \hat{q}_\mu, \end{aligned} \quad (39)$$

$$\Omega_{\tilde{\nu}} = \sum_i \frac{\lambda_{ijk} \lambda_{i32}^{I*}}{8m_{\tilde{\nu}_{iL}}^2} \left[-\frac{i}{2} \frac{A_0^{B \rightarrow K^*}(\hat{s})}{\bar{m}_b + \bar{m}_s} \lambda^{1/2} m_B^2 \right], \quad (40)$$

$$\Omega'_{\tilde{\nu}} = \sum_i \frac{\lambda_{ikj}^* \lambda'_{i23}}{8m_{\tilde{\nu}_{iL}}^2} \left[\frac{i}{2} \frac{A_0^{B \rightarrow K^*}(\hat{s})}{\bar{m}_b + \bar{m}_s} \lambda^{1/2} m_B^2 \right], \quad (41)$$

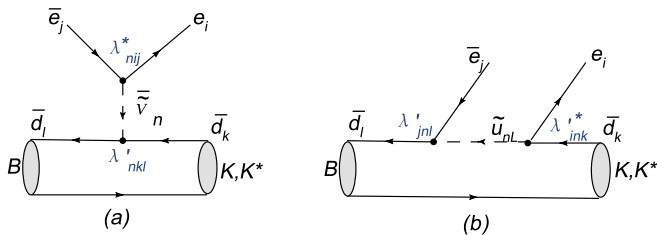


FIG. 1 (color online). The RPV contributions to $B \rightarrow K^{(*)} \ell^+ \ell^-$ due to sneutrino and squark exchange.

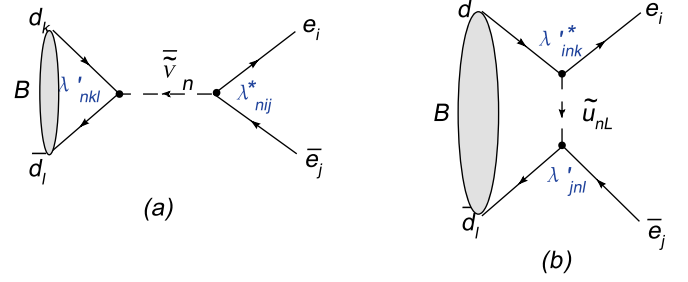


FIG. 2 (color online). The RPV contributions to $B_s \rightarrow \ell^+ \ell^-$ due to sneutrino and squark exchange.

and the auxiliary functions are given as

$$I(\hat{s}) = \sum_i \frac{\lambda'_{ji3} \lambda_{ki2}^{I*}}{8m_{\tilde{u}_{iL}}^2} \left[\frac{2V^{B \rightarrow K^*}(\hat{s})}{m_B + m_{K^*}} m_B^2 \right], \quad (42)$$

$$J(\hat{s}) = \sum_i \frac{\lambda'_{ji3} \lambda_{ki2}^{I*}}{8m_{\tilde{u}_{iL}}^2} [-(m_B + m_{K^*}) A_1^{B \rightarrow K^*}(\hat{s})], \quad (43)$$

$$K(\hat{s}) = \sum_i \frac{\lambda'_{ji3} \lambda_{ki2}^{I*}}{8m_{\tilde{u}_{iL}}^2} \left[\frac{A_2^{B \rightarrow K^*}(\hat{s})}{m_B + m_{K^*}} m_B^2 \right], \quad (44)$$

$$L(\hat{s}) = \sum_i \frac{\lambda'_{ji3} \lambda_{ki2}^{I*}}{8m_{\tilde{u}_{iL}}^2} \left[\frac{2m_{K^*}}{\hat{s}} (A_3^{B \rightarrow K^*}(\hat{s}) - A_0^{B \rightarrow K^*}(\hat{s})) \right]. \quad (45)$$

For $B_s \rightarrow \ell^+ \ell^-$, the RPV amplitude is

$$\begin{aligned} \mathcal{M}^{\mathcal{R}_p}(B_s \rightarrow \ell^+ \ell^-) = & \Lambda_{\tilde{u}} (\bar{\ell}_k \not{p}_B (1 - \gamma_5) \ell_j) \\ & + \Lambda_{\tilde{\nu}} (\bar{\ell}_k (1 - \gamma_5) \ell_j) \\ & + \Lambda'_{\tilde{\nu}} (\bar{\ell}_k (1 + \gamma_5) \ell_j), \end{aligned} \quad (46)$$

with

$$\Lambda_{\tilde{u}} = \sum_i \frac{\lambda'_{ji3} \lambda_{ki2}^{I*}}{8m_{\tilde{u}_{iL}}^2} (-if_{B_s}), \quad (47)$$

$$\Lambda_{\tilde{\nu}} = \sum_i \frac{\lambda_{ijk} \lambda_{i32}^{I*}}{8m_{\tilde{\nu}_{iL}}^2} (-if_{B_s} \mu_{B_s}), \quad (48)$$

$$\Lambda'_{\tilde{\nu}} = \sum_i \frac{\lambda_{ikj}^* \lambda'_{i23}}{8m_{\tilde{\nu}_{iL}}^2} (if_{B_s} \mu_{B_s}), \quad (49)$$

and $\mu_{B_s} \equiv \frac{m_{B_s}^2}{\bar{m}_b + \bar{m}_s}$.

The RPV couplings can be complex in general; we write their products as

$$\begin{aligned} \Lambda_{ijk} \Lambda_{lmn}^* &= |\Lambda_{ijk} \Lambda_{lmn}^*| e^{i\phi_{\mathcal{R}_p}}, \\ \Lambda_{ijk}^* \Lambda_{lmn} &= |\Lambda_{ijk} \Lambda_{lmn}^*| e^{-i\phi_{\mathcal{R}_p}}, \end{aligned} \quad (50)$$

where the RPV coupling constant $\Lambda \in \{\lambda, \lambda'\}$, and $\phi_{\mathcal{R}_p}$ is the RPV weak phase.

C. The branching ratios with RPV contributions

With these formulae in Secs. II A and II B, we can obtain the total double differential decay branching ratios of the

decays $B \rightarrow K^{(*)} \ell^+ \ell^-$,

$$\frac{d^2 \mathcal{B}_{\text{All}}^{K^{(*)}}}{d\hat{s}d\hat{u}} = \frac{d^2 \mathcal{B}_{\text{SM}}^{K^{(*)}}}{d\hat{s}d\hat{u}} + \frac{d^2 \mathcal{B}_{\hat{u}}^{K^{(*)}}}{d\hat{s}d\hat{u}} + \frac{d^2 \mathcal{B}_{\hat{\nu}}^{K^{(*)}}}{d\hat{s}d\hat{u}} + \frac{d^2 \mathcal{B}_{\hat{\nu}}^{\prime K^{(*)}}}{d\hat{s}d\hat{u}}. \quad (51)$$

Since we will only consider one RPV coupling product contributes at one time, we have neglected the interferences between different RPV coupling products, but kept their interferences with the SM amplitude, as shown in the following equations.

For the $B \rightarrow K \ell^+ \ell^-$ decay,

$$\begin{aligned} \frac{d^2 \mathcal{B}_{\hat{u}}^K}{d\hat{s}d\hat{u}} &= \tau_B \frac{m_B^4}{2^7 \pi^3} \{ \text{Re}(WA' \Delta_{\hat{u}}^*) (\lambda - \hat{u}^2) \\ &+ \text{Re}(WC' \Delta_{\hat{u}}^*) [-(\lambda - \hat{u}^2) - 4\hat{m}_\ell^2 (2 + 2\hat{m}_K^2 - \hat{s})] \\ &+ \text{Re}(WD' \Delta_{\hat{u}}^*) [-4\hat{m}_\ell^2 (1 - \hat{m}_K^2)] \\ &+ |\Delta_{\hat{u}}|^2 m_B [\lambda - \hat{u} + 2\hat{m}_\ell^2 (2 + 2\hat{m}_K^2 - \hat{s})] \}, \quad (52) \end{aligned}$$

$$\begin{aligned} \frac{d^2 \mathcal{B}_{\hat{\nu}}^K}{d\hat{s}d\hat{u}} &= \tau_B \frac{m_B^3}{2^7 \pi^3} \{ \text{Re}(WA' \Delta_{\hat{\nu}}^*) (2\hat{m}_\ell \hat{u}) \\ &+ \text{Re}(WC' \Delta_{\hat{\nu}}^*) (1 - \hat{m}_K^2) (-2\hat{m}_\ell) \\ &+ \text{Re}(WD' \Delta_{\hat{\nu}}^*) (-2\hat{m}_\ell \hat{s}) \\ &+ |\Delta_{\hat{\nu}}|^2 (\hat{s} - 2\hat{m}_\ell^2) \}, \quad (53) \end{aligned}$$

$$\begin{aligned} \frac{d^2 \mathcal{B}_{\hat{\nu}}^{\prime K}}{d\hat{s}d\hat{u}} &= \tau_B \frac{m_B^3}{2^7 \pi^3} \{ \text{Re}(WA' \Delta_{\hat{\nu}}^*) (2\hat{m}_\ell \hat{u}) \\ &+ \text{Re}(WC' \Delta_{\hat{\nu}}^*) (1 - \hat{m}_K^2) (2\hat{m}_\ell) \\ &+ \text{Re}(WD' \Delta_{\hat{\nu}}^*) (2\hat{m}_\ell \hat{s}) + |\Delta_{\hat{\nu}}|^2 (\hat{s} - 2\hat{m}_\ell^2) \}, \quad (54) \end{aligned}$$

with $W = -\frac{G_F \alpha_e}{2\sqrt{2}\pi} V_{ts}^* V_{tb} m_B$.

For the $B \rightarrow K^* \ell^+ \ell^-$ decay, we have

$$\begin{aligned} \frac{d^2 \mathcal{B}_{\hat{u}}^{K^*}}{d\hat{s}d\hat{u}} &= \tau_B \frac{m_B^3}{2^9 \pi^3} \left\{ \text{Re}(WAI^*) [\hat{s}(\lambda + \hat{u}^2) + 4\hat{m}_\ell^2 \lambda] - \text{Re}(WEI^*) [\hat{s}(\lambda + \hat{u}^2) - 4\hat{m}_\ell^2 \lambda] + |I|^2 [\hat{s}(\lambda + \hat{u}^2)] \right. \\ &+ 4\hat{s} \hat{u} [\text{Re}(WAJ^*) + \text{Re}(WBI^*) - \text{Re}(WEJ^*) - \text{Re}(WFI^*) + 2\text{Re}(IJ^*)] \\ &+ \frac{1}{\hat{m}_{K^*}^2} [\text{Re}(WBJ^*) (\lambda - \hat{u}^2 + 8\hat{m}_{K^*}^2 (\hat{s} + 2\hat{m}_\ell^2)) - \text{Re}(WFJ^*) (\lambda - \hat{u}^2 + 8\hat{m}_{K^*}^2 (\hat{s} - 4\hat{m}_\ell^2)) \\ &+ |J|^2 (\lambda - \hat{u}^2 + 8\hat{m}_{K^*}^2 (\hat{s} - \hat{m}_\ell^2)) - \text{Re}(WBK^*) (\lambda - \hat{u}^2) (1 - \hat{m}_{K^*}^2 - \hat{s}) + \text{Re}(WFK^*) ((\lambda - \hat{u}^2) (1 - \hat{m}_{K^*}^2 - \hat{s}) + 4\hat{m}_\ell^2 \lambda) \\ &- 2\text{Re}(JK^*) ((\lambda - \hat{u}^2) (1 - \hat{m}_{K^*}^2 - \hat{s}) + 2\hat{m}_\ell^2 \lambda)] + \frac{\lambda}{\hat{m}_{K^*}^2} [\text{Re}(WCK^*) (\lambda - \hat{u}^2) \\ &- \text{Re}(W GK^*) (\lambda - \hat{u}^2 + 4\hat{m}_\ell^2 (2 + 2\hat{m}_{K^*}^2 - \hat{s})) + |K|^2 (\lambda - \hat{u}^2 + 2\hat{m}_\ell^2 (2 + 2\hat{m}_{K^*}^2 - \hat{s}))] \\ &\left. + \frac{4\hat{m}_\ell^2}{\hat{m}_{K^*}^2} \lambda [-\text{Re}(WHL^*) \hat{s} + |L|^2 \hat{s}/2 + \text{Re}(WFL^*) - \text{Re}(JL^*) - \text{Re}(WGL^*) (1 - \hat{m}_{K^*}^2) + \text{Re}(KL^*) (1 - \hat{m}_{K^*}^2)] \right\}, \quad (55) \end{aligned}$$

$$\begin{aligned} \frac{d^2 \mathcal{B}_{\hat{\nu}}^{K^*}}{d\hat{s}d\hat{u}} &= \tau_B \frac{m_B^3}{2^7 \pi^3} \left\{ -\frac{\hat{m}_\ell^2}{\hat{m}_{K^*}^2} [\text{Im}(WB\Omega_{\hat{\nu}}^*) \right. \\ &\cdot (\lambda^{-1/2} \hat{u} (1 - \hat{m}_{K^*}^2 - \hat{s})) + \text{Im}(WC\Omega_{\hat{\nu}}^*) \lambda^{1/2} \hat{u} \\ &+ \text{Im}(WF\Omega_{\hat{\nu}}^*) \lambda^{1/2} - \text{Im}(WG\Omega_{\hat{\nu}}^*) \lambda^{1/2} (1 - \hat{m}_{K^*}^2)] \\ &\left. + |\Omega_{\hat{\nu}}|^2 (\hat{s} - 2\hat{m}_\ell^2) \right\}, \quad (56) \end{aligned}$$

$$\begin{aligned} \frac{d^2 \mathcal{B}_{\hat{\nu}}^{\prime K^*}}{d\hat{s}d\hat{u}} &= \tau_B \frac{m_B^3}{2^7 \pi^3} \left\{ -\frac{\hat{m}_\ell^2}{\hat{m}_{K^*}^2} [\text{Im}(WB\Omega_{\hat{\nu}}^*) \right. \\ &\cdot (\lambda^{-1/2} \hat{u} (1 - \hat{m}_{K^*}^2 - \hat{s})) + \text{Im}(WC\Omega_{\hat{\nu}}^*) \lambda^{1/2} \hat{u} \\ &- \text{Im}(WF\Omega_{\hat{\nu}}^*) \lambda^{1/2} + \text{Im}(WG\Omega_{\hat{\nu}}^*) \lambda^{1/2} (1 - \hat{m}_{K^*}^2)] \\ &\left. + |\Omega_{\hat{\nu}}^{\prime}|^2 (\hat{s} - 2\hat{m}_\ell^2) \right\}. \quad (57) \end{aligned}$$

From the total double differential branching ratios, we can get the normalized forward-backward asymmetries \mathcal{A}_{FB} [1]

$$\begin{aligned} \mathcal{A}_{\text{FB}}(B \rightarrow K^{(*)} \ell^+ \ell^-) &= \int d\hat{s} \frac{\int_{-1}^{+1} \frac{d^2 \mathcal{B}(B \rightarrow K^{(*)} \ell^+ \ell^-)}{d\hat{s}d\cos\theta} \text{sign}(\cos\theta) d\cos\theta}{\int_{-1}^{+1} \frac{d^2 \mathcal{B}(B \rightarrow K^{(*)} \ell^+ \ell^-)}{d\hat{s}d\cos\theta} d\cos\theta}. \quad (58) \end{aligned}$$

In the SM, the \mathcal{A}_{FB} vanishes in $B \rightarrow K \ell^+ \ell^-$ decays as shown by Eq. (27), since there is no term containing \hat{u} with an odd power. The RPV effect via the squark exchange on $\mathcal{A}_{\text{FB}}(B \rightarrow K \ell^+ \ell^-)$ also vanishes for the same reason as shown by Eq. (52).

The total decay branching ratios of the pure leptonic B_s decays are calculated to be

$$\begin{aligned}
\mathcal{B}(B_s \rightarrow \ell^+ \ell^-) &= \mathcal{B}^{\text{SM}}(B_s \rightarrow \ell^+ \ell^-) \\
&\times \left\{ 1 + \frac{1}{|h_{\text{SM}}|^2} [2 \text{Re}(h_{\text{SM}} \Lambda_{\tilde{u}}^*) + |\Lambda_{\tilde{u}}|^2] \right. \\
&+ \frac{1}{|h_{\text{SM}}|^2} \left[\text{Re}(h_{\text{SM}} \Lambda_{\tilde{\nu}}^*) \frac{1}{m_\ell} \right. \\
&+ |\Lambda_{\tilde{\nu}}|^2 \left. \left(\frac{1}{2m_\ell^2} - \frac{1}{m_{B_s}^2} \right) \right] \\
&+ \frac{1}{|h_{\text{SM}}|^2} \left[-\text{Re}(h_{\text{SM}} \Lambda_{\tilde{\nu}}^{*'}) \frac{1}{m_\ell} \right. \\
&+ |\Lambda_{\tilde{\nu}}'|^2 \left. \left(\frac{1}{2m_\ell^2} - \frac{1}{m_{B_s}^2} \right) \right] \left. \right\}. \quad (59)
\end{aligned}$$

From this equation, we can see that $\mathcal{B}(B_s \rightarrow \ell^+ \ell^-)$ could be enhanced very much by the s -channel RPV sneutrino exchange, but not by the t -channel squark exchange.

III. NUMERICAL RESULTS AND ANALYSIS

Now we are ready to present our numerical results and analysis. First, we will show our estimations and compare them with the relevant experimental data of $\mathcal{B}(B \rightarrow K^{(*)} \ell^+ \ell^-)$ and upper limits of $\mathcal{B}(B_s \rightarrow \ell^+ \ell^-)$. Then, we will consider the RPV effects to constrain the relevant RPV couplings. In addition, using the constrained parameter spaces, we will give the RPV SUSY predictions for $\mathcal{B}(B_s \rightarrow \ell^+ \ell^-)$ and $\mathcal{A}_{\text{FB}}(B \rightarrow K^{(*)} \ell^+ \ell^-)$, which have not been well measured yet.

For the form factors involving the $B \rightarrow K^{(*)}$ transitions, we will use the recently light-cone QCD sum rules (LCSRs) results [23], which are renewed with radiative corrections to the leading twist wave functions and SU(3) breaking effects. For the q^2 dependence of the form factors, they can be parametrized in terms of simple formulae with two or three parameters. The form factors V , A_0 , and T_1 are parametrized by

$$F(\hat{s}) = \frac{r_1}{1 - \hat{s}/\hat{m}_R^2} + \frac{r_2}{1 - \hat{s}/\hat{m}_{\text{fit}}^2}. \quad (60)$$

For the form factors A_2 , \tilde{T}_3 , f_+ , and f_T , it is more appropriate to expand to second order around the pole, yielding

$$F(\hat{s}) = \frac{r_1}{1 - \hat{s}/\hat{m}^2} + \frac{r_2}{(1 - \hat{s}/\hat{m}^2)^2}, \quad (61)$$

where $\hat{m} = \hat{m}_{\text{fit}}$ for A_2 and \tilde{T}_3 , and $\hat{m} = \hat{m}_R$ for f_+ and f_T . The fit formula for A_1 , T_2 , and f_0 is

$$F(\hat{s}) = \frac{r_2}{1 - \hat{s}/\hat{m}_{\text{fit}}^2}. \quad (62)$$

The form factor T_3 can be obtained by $T_3(\hat{s}) = \frac{1 - \hat{m}_{K^*}}{\hat{s}} \times [\tilde{T}_3(\hat{s}) - T_2(\hat{s})]$. All the corresponding parameters for these form factors are collected in Table I. In the following numerical data analyses, the uncertainties induced by $F(0)$ [23] are also considered.

TABLE I. Fit for form factors involving the $B \rightarrow K^{(*)}$ transitions valid for general q^2 [23].

$F(\hat{s})$	$F(0)$	Δ_{tot}	r_1	m_R^2	r_2	m_{fit}^2	fit Eq.
$f_+^{B \rightarrow K}$	0.331	0.041	0.162	5.41^2	0.173		(61)
$f_T^{B \rightarrow K}$	0.358	0.037	0.161	5.41^2	0.198		(61)
$f_0^{B \rightarrow K}$	0.331	0.041			0.330	37.46	(62)
$V^{B \rightarrow K^*}$	0.411	0.033	0.923	5.32^2	-0.511	49.40	(60)
$A_0^{B \rightarrow K^*}$	0.374	0.033	1.364	5.28^2	-0.990	36.78	(60)
$A_1^{B \rightarrow K^*}$	0.292	0.028			0.290	40.38	(62)
$A_2^{B \rightarrow K^*}$	0.259	0.027	-0.084		0.342	52.00	(61)
$T_1^{B \rightarrow K^*}$	0.333	0.028	0.823	5.32^2	-0.491	46.31	(60)
$T_2^{B \rightarrow K^*}$	0.333	0.028			0.333	41.41	(62)
$\tilde{T}_3^{B \rightarrow K^*}$	0.333	0.028	-0.036		0.368	48.10	(61)

The other input parameters and the experimental data are collected in Tables II and III, respectively. In our numerical results, if not specified, we will study physics observables in the region $s > 0.1 \text{ GeV}^2$, and use the input parameters and the experimental data which are varied randomly within 1σ and 2σ variance, respectively. We assume that only one sfermion contributes at one time with a mass of 100 GeV. As for other values of the sfermion masses, the bounds on the couplings in this paper can be easily obtained by scaling them with factor $\tilde{f}^2 \equiv (\frac{m_{\tilde{f}}}{100 \text{ GeV}})^2$.

The branching ratios in the SM estimated with the central values of the input parameters are presented in Table III, and the relevant experimental data and upper limits [1,2,4,27,29] are listed for comparison. From Table III, we can find that the branching ratios of the semileptonic decays are roughly consistent with the SM predictions. So, there are still windows, however limited, for RPV contributions.

We now turn to the RPV effects. There are six RPV coupling products contributing to four $B \rightarrow K^{(*)} \ell^+ \ell^-$ and two $B_s \rightarrow \ell^+ \ell^-$ decay modes. We use the experimental

TABLE II. Default values of the input parameters and the $\pm 1\sigma$ error bars for the sensitive parameters used in our numerical calculations.

$m_{B_s} = 5.370 \text{ GeV}$, $m_{B_d} = 5.279 \text{ GeV}$, $m_{B_u} = 5.279 \text{ GeV}$, [27]
$m_W = 80.425 \text{ GeV}$, $m_{K^\pm} = 0.494 \text{ GeV}$, $m_{K^0} = 0.498 \text{ GeV}$,
$m_{K^{*\pm}} = 0.892 \text{ GeV}$, $m_{K^{*0}} = 0.896 \text{ GeV}$, $\tilde{m}_b(\tilde{m}_b) = (4.20 \pm 0.07) \text{ GeV}$,
$\tilde{m}_s(2 \text{ GeV}) = (0.095 \pm 0.025) \text{ GeV}$,
$\tilde{m}_u(2 \text{ GeV}) = 0.0015 \sim 0.003 \text{ GeV}$, $\tilde{m}_d(2 \text{ GeV}) = 0.003 \sim 0.007 \text{ GeV}$,
$m_e = 0.511 \times 10^{-3} \text{ GeV}$, $m_\mu = 0.106 \text{ GeV}$,
$m_{r,\text{pole}} = 174.2 \pm 3.3 \text{ GeV}$.
$\tau_{B_s} = (1.466 \pm 0.059) ps$, $\tau_{B_d} = (1.530 \pm 0.009) ps$, $\tau_{B_u} = [27]$
$(1.638 \pm 0.011) ps$.
$ V_{tb} \approx 0.99910$, $ V_{ts} = 0.04161_{-0.00078}^{+0.00012}$. [27]
$\sin^2 \theta_W = 0.22306$, $\alpha_e = 1/137$. [27]
$f_{B_s} = 0.230 \pm 0.030 \text{ GeV}$. [28]

TABLE III. The SM predictions and the experimental data for $B \rightarrow K^{(*)}\ell^+\ell^-$ and the upper limits for $B \rightarrow \ell^+\ell^-$ [1,2,4,27,29].

	SM prediction value	Experimental data
$\mathcal{B}(B \rightarrow K\mu^+\mu^-)$	0.610×10^{-6}	$(0.561^{+0.066}_{-0.061}) \times 10^{-6}$
$\mathcal{B}(B \rightarrow Ke^+e^-)$	0.610×10^{-6}	$(0.380^{+0.073}_{-0.067}) \times 10^{-6}$
$\mathcal{B}(B \rightarrow K^*\mu^+\mu^-)$	1.27×10^{-6}	$(1.44 \pm 0.23) \times 10^{-6}$
$\mathcal{B}(B \rightarrow K^*e^+e^-)$	1.29×10^{-6}	$(1.25 \pm 0.27) \times 10^{-6}$
$\mathcal{B}(B_s \rightarrow \mu^+\mu^-)$	3.72×10^{-9}	$<1.0 \times 10^{-7}$ (95% C.L.)
$\mathcal{B}(B_s \rightarrow e^+e^-)$	8.70×10^{-14}	$<5.4 \times 10^{-5}$ (90% C.L.)

 TABLE IV. Bounds for the relevant RPV coupling products by $B \rightarrow K^{(*)}\ell^+\ell^-$ and $B_s \rightarrow \ell^+\ell^-$ decays for 100 GeV sfermions, and previous bounds are listed for comparison.

Couplings	Bounds [Processes]	Previous bounds [Processes]
$ \lambda'_{i13}\lambda'_{i12} $	$\leq 4.7 \times 10^{-5}[B \rightarrow K^{(*)}e^+e^-]$	$\leq 9.6 \times 10^{-5}[B \rightarrow Ke^+e^-]$ [22]
$ \lambda'_{i11}\lambda'_{i32} $	$\leq 2.3 \times 10^{-5}[B \rightarrow K^{(*)}e^+e^-]$	$\leq 1.5 \times 10^{-3}$ [30]
$ \lambda'_{i11}\lambda'_{i23} $	$\leq 2.3 \times 10^{-5}[B \rightarrow K^{(*)}e^+e^-]$	$\leq 1.9 \times 10^{-4}$ [30]
$ \lambda'_{2i3}\lambda'_{2i2} $	$\leq 4.6 \times 10^{-5}$ $\begin{matrix} [B_s \rightarrow \mu^+\mu^-] \\ [B \rightarrow K^{(*)}\mu^+\mu^-] \end{matrix}$	$\begin{matrix} \leq 9.7 \times 10^{-5} [B_s \rightarrow \mu^+\mu^-] \\ \leq 3.9 \times 10^{-3} [B \rightarrow K\mu^+\mu^-] \end{matrix}$ [22]
$ \lambda'_{i22}\lambda'_{i32} $	$\leq 1.8 \times 10^{-5}$ $\begin{matrix} [B_s \rightarrow \mu^+\mu^-] \\ [B \rightarrow K^{(*)}\mu^+\mu^-] \end{matrix}$	$\leq 2.7 \times 10^{-5}[B \rightarrow K\mu^+\mu^-]$ [22]
$ \lambda'_{i22}\lambda'_{i23} $	$\leq 1.7 \times 10^{-5}$ $\begin{matrix} [B_s \rightarrow \mu^+\mu^-] \\ [B \rightarrow K^{(*)}\mu^+\mu^-] \end{matrix}$	$\leq 2.7 \times 10^{-5}[B \rightarrow K\mu^+\mu^-]$ [22]

data of the branching ratios listed in Table III to constrain the relevant RPV coupling products.

For the RPV couplings $\lambda'_{i11}\lambda'_{i32}$ and $\lambda'_{i11}\lambda'_{i23}$, since their RPV weak phases are found to have very small contribu-

tions to the physical observables, we take their RPV weak phases to be free, and only give the upper limits for their modulus which are listed in Table IV. In Fig. 3, we present our bounds on the other four RPV coupling products.

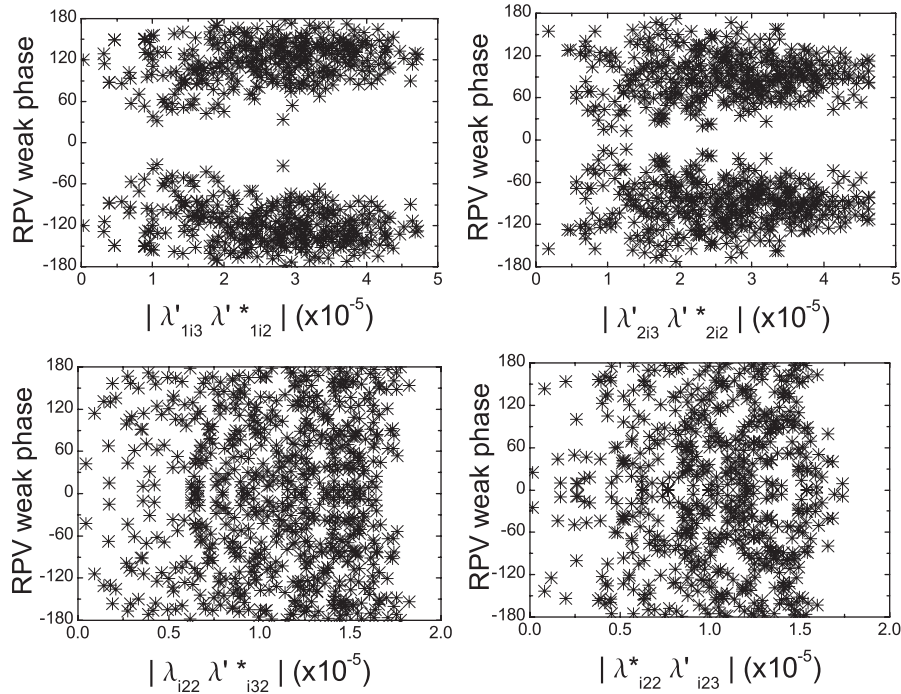


FIG. 3. The allowed parameter spaces for the relevant RPV coupling products constrained by the measurements listed in Table IV, and the RPV weak phase is given in degree.

TABLE V. The theoretical predictions for $\mathcal{B}(B_s \rightarrow \ell^+ \ell^-)$ and $\mathcal{A}_{\text{FB}}(B \rightarrow K^{(*)} \ell^+ \ell^-)$ in the SM and the RPV SUSY. The RPV SUSY predictions are obtained by the constrained regions of the different RPV coupling products. The index $g = 1$ and 2 for $\ell = e$ and μ , respectively.

	SM value	$\lambda'_{gi3} \lambda_{gi2}^*$	$\lambda_{igg} \lambda_{i32}^*$	$\lambda_{igg}^* \lambda'_{i23}$
$\mathcal{B}(B_s \rightarrow e^+ e^-)$	$[5.9, 11.2] \times 10^{-14}$	$[5.3, 17.0] \times 10^{-14}$	$\leq 2.2 \times 10^{-7}$	$\leq 2.2 \times 10^{-7}$
$\mathcal{A}_{\text{FB}}(B \rightarrow Ke^+ e^-)$	0	0	$[-4.1, 5.0] \times 10^{-5}$	$[-4.0, 5.0] \times 10^{-5}$
$\mathcal{A}_{\text{FB}}(B \rightarrow K^* e^+ e^-)$	[0.12, 0.18]	[0.00, 0.29]	[0.12, 0.18]	[0.13, 0.18]
$\mathcal{B}(B_s \rightarrow \mu^+ \mu^-)$	$[2.7, 4.8] \times 10^{-9}$	$[2.1, 6.8] \times 10^{-9}$	$< 1.0 \times 10^{-7}$	$< 1.0 \times 10^{-7}$
$\mathcal{A}_{\text{FB}}(B \rightarrow K\mu^+ \mu^-)$	0	0	$[-7.0, 6.9] \times 10^{-3}$	$[-6.8, 7.0] \times 10^{-3}$
$\mathcal{A}_{\text{FB}}(B \rightarrow K^* \mu^+ \mu^-)$	[0.13, 0.18]	[0.02, 0.76]	[0.13, 0.18]	[0.013, 0.18]

From Fig. 3, we find that every RPV weak phase is not constrained so much, but the modulus of the relevant RPV coupling products are tightly upper limited. The upper limits for the relevant RPV coupling products by $B \rightarrow K^{(*)} \ell^+ \ell^-$ and $B_s \rightarrow \ell^+ \ell^-$ decays are summarized in Table IV. For comparison, the existing bounds on these quadric coupling products [22,30] are also listed. From Table IV, one can find that our bounds are more restricted than the previous ones. It is also noted that the previous bounds of $|\lambda_{i11} \lambda_{i32}^*|$ and $|\lambda_{i11}^* \lambda'_{i23}|$ are obtained at the M_{GUT} scale in the RPV mSUGRA model [30].

Using the constrained parameter spaces shown in Table IV and Fig. 3, we can predict the RPV effects on the other quantities which have not been well measured yet in these processes. We perform a scan over the input parameters and the new constrained RPV coupling spaces to get the allowed ranges for $\mathcal{B}(B_s \rightarrow \ell^+ \ell^-)$ and $\mathcal{A}_{\text{FB}}(B \rightarrow K^{(*)} \ell^+ \ell^-)$ with the different RPV coupling products. Our numerical results are summarized in Table V.

From Table V, we can find some salient features of the numerical results.

- (i) As shown by Fig. 2(b), the contributions of $\lambda'_{i13} \lambda_{i2}^*$ and $\lambda'_{i23} \lambda_{i2}^*$ to $\mathcal{B}(B_s \rightarrow e^+ e^-)$ and $\mathcal{B}(B_s \rightarrow \mu^+ \mu^-)$, respectively, arise from t -channel squark exchange. After Fierz transformation, the effective Hamiltonian due to the t -channel squark exchange is proportional to $(\bar{s} \gamma^\mu P_R b)(\bar{\ell} \gamma_\mu P_L \ell)$, which the contribution to $\mathcal{B}(B_s \rightarrow \ell^+ \ell^-)$ is suppressed by m_ℓ^2/m_B^2 due to helicity suppression. Therefore $\mathcal{B}(B_s \rightarrow e^+ e^-, \mu^+ \mu^-)$ will not be enhanced so much by the t -channel squark exchanging RPV contributions. However, the effective Hamiltonian of s -channel sneutrino exchange would be $(\bar{s}(1 \pm \gamma_5)b) \times (\bar{\ell}(1 \mp \gamma_5)\ell)$, whose contributions are not suppressed by m_ℓ^2/m_B^2 . So that, both $\mathcal{B}(B_s \rightarrow e^+ e^-)$ and $\mathcal{B}(B_s \rightarrow \mu^+ \mu^-)$ could be enhanced to order 10^{-7} by $\lambda_{i11} \lambda_{i32}^* (\lambda_{i11}^* \lambda'_{i23})$ and $\lambda_{i22} \lambda_{i32}^* (\lambda_{i22}^* \lambda'_{i23})$, respectively.
- (ii) Both $\mathcal{A}_{\text{FB}}(B \rightarrow Ke^+ e^-)$ and $\mathcal{A}_{\text{FB}}(B \rightarrow K\mu^+ \mu^-)$ are zero in the SM. The RPV contributions to the asymmetries due to squark exchange are also zero,

while the sneutrino exchange RPV contributions are too small to be accessible at LHC.

- (iii) It is interesting to note that the RPV squark exchange contributions have significant impacts on $\mathcal{A}_{\text{FB}}(B \rightarrow K^* e^+ e^-)$ and $\mathcal{A}_{\text{FB}}(B \rightarrow K^* \mu^+ \mu^-)$. However, the sneutrino exchange have negligible effects on $\mathcal{A}_{\text{FB}}(B \rightarrow K^* e^+ e^-)$ and $\mathcal{A}_{\text{FB}}(B \rightarrow K^* \mu^+ \mu^-)$.

Recently, the *BABAR* Collaboration [1] has measured

$$\mathcal{A}_{\text{FB}}(B^+ \rightarrow K^+ \ell^+ \ell^-)_{(s>0.1 \text{ GeV}^2)} = 0.15_{-0.23}^{+0.21} \pm 0.08, \quad (63)$$

$$\mathcal{A}_{\text{FB}}(B \rightarrow K^* \ell^+ \ell^-)_{(s>0.1 \text{ GeV}^2)} \geq 0.55(95\% \text{C.L.}), \quad (64)$$

and Belle Collaboration has measured the integrated forward-backward asymmetries $\tilde{\mathcal{A}}_{\text{FB}}$ [3]

$$\tilde{\mathcal{A}}_{\text{FB}}(B^+ \rightarrow K^+ \ell^+ \ell^-) = 0.10 \pm 0.14 \pm 0.01, \quad (65)$$

$$\tilde{\mathcal{A}}_{\text{FB}}(B \rightarrow K^* \ell^+ \ell^-) = 0.50 \pm 0.15 \pm 0.02, \quad (66)$$

where $\tilde{\mathcal{A}}_{\text{FB}}$ is slightly different from \mathcal{A}_{FB} , and defined by

$$\begin{aligned} \tilde{\mathcal{A}}_{\text{FB}}(B \rightarrow K^{(*)} \ell^+ \ell^-) &= \frac{\int \frac{d^2 \mathcal{B}(B \rightarrow K^{(*)} \ell^+ \ell^-)}{d \cos \theta d \hat{s}} \text{sign}(\cos \theta) d \cos \theta d \hat{s}}{\int \frac{d^2 \mathcal{B}(B \rightarrow K^{(*)} \ell^+ \ell^-)}{d \cos \theta d \hat{s}} d \cos \theta d \hat{s}}. \end{aligned} \quad (67)$$

We find that the SM predictions for $\mathcal{A}_{\text{FB}}(B \rightarrow K^* \ell^+ \ell^-)$ are consistent with both the measurements within error bars.

In Figs. 4–9, we present correlations between the physical observable \mathcal{B} , \mathcal{A}_{FB} and the parameter spaces of the different RPV coupling products by the three-dimensional scatter plots and the two-dimensional scatter plots, respectively. The dilepton invariant mass distribution and the normalized forward-backward asymmetry are given with VMD contribution excluded in terms of $d\mathcal{B}/d\hat{s}$ and $d\mathcal{A}_{\text{FB}}/d\hat{s}$, and included in $d\mathcal{B}'/d\hat{s}$ and $d\mathcal{A}'_{\text{FB}}/d\hat{s}$, respectively. From Figs. 4–9, one can find the correlations of these physical observables with RPV coupling products. In Figs. 5 and 6, since the influences of the RPV weak phases are very small, we take the RPV weak phases randomly

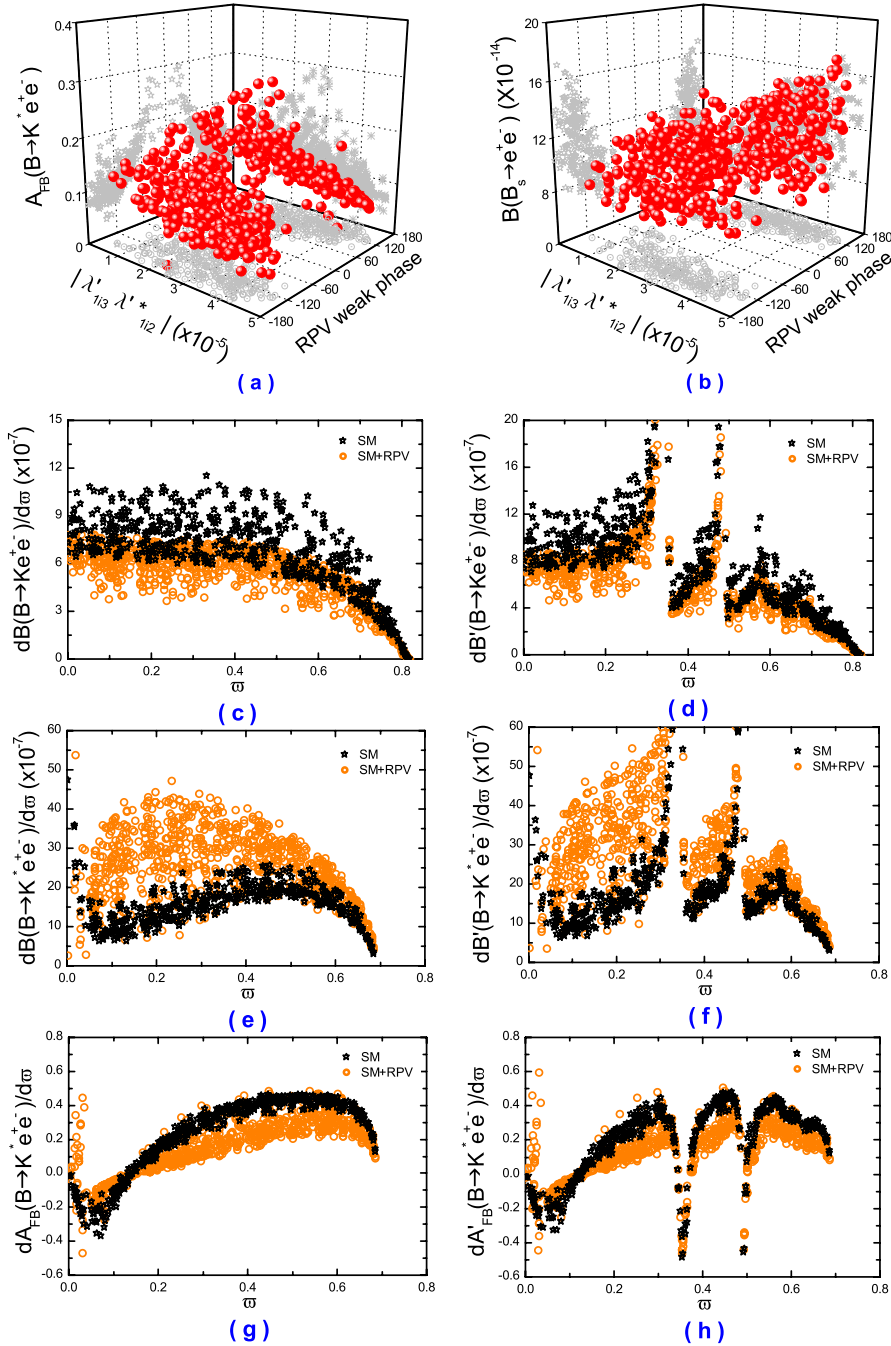


FIG. 4 (color online). The effects of RPV coupling $\lambda'_{1i3}\lambda_{1i2}^{I*}$ due to the squark exchange in $B \rightarrow K^{(*)}e^+e^-$ and $B_s \rightarrow e^+e^-$ decays. The primed observables are given with $\psi(nS)$ VMD contributions, and ϖ denote \hat{s} .

varied in $[-\pi, \pi]$ and only give the change trends of the physical observables with the relative modulus in the two-dimensional scatter plots.

At first, we will discuss plots of Fig. 4 in detail. The three-dimensional scatter plot Fig. 4(a) shows $\mathcal{A}_{\text{FB}}(B \rightarrow K^*e^+e^-)$ correlated with $|\lambda'_{1i3}\lambda_{1i2}^{I*}|$ and its phase $\phi_{\mathcal{R}_p}$. We also give projections on three vertical planes, where the $|\lambda'_{1i3}\lambda_{1i2}^{I*}|-\phi_{\mathcal{R}_p}$ plane displays the constrained regions of

$\lambda'_{1i3}\lambda_{1i2}^{I*}$ as the first plot of Fig. 3. It is shown that $\mathcal{A}_{\text{FB}}(B \rightarrow K^*e^+e^-)$ is decreasing with $|\lambda'_{1i3}\lambda_{1i2}^{I*}|$ on the $\mathcal{A}_{\text{FB}}(B \rightarrow K^*e^+e^-)-|\lambda'_{1i3}\lambda_{1i2}^{I*}|$ plane. From the $\mathcal{A}_{\text{FB}}(B \rightarrow K^*e^+e^-)-\phi_{\mathcal{R}_p}$ plane, we can see that $\mathcal{A}_{\text{FB}}(B \rightarrow K^*e^+e^-)$ is decreasing with $|\phi_{\mathcal{R}_p}|$. The recent measurement of $\mathcal{A}_{\text{FB}}(B \rightarrow K^*\ell^+\ell^-)$ favors $|\lambda'_{1i3}\lambda_{1i2}^{I*}| \sim (2 \sim 4) \times 10^{-5}$ with small $\phi_{\mathcal{R}_p}$. However $B_s \rightarrow e^+e^-$ is remained inaccessible at LHC. From plots Fig. 4(c)–

4(h), we can find that the theoretical uncertainties in the calculation of the SM contributions are still very large, nevertheless, for $d\mathcal{B}(B \rightarrow K^{(*)}e^+e^-)/d\hat{s}$ and $d\mathcal{A}_{\text{FB}}(B \rightarrow K^*e^+e^-)/d\hat{s}$, the $\lambda'_{i13}\lambda_{i12}^*$ contributions are distinguishable from the hadronic uncertainties.

Figures 5 and 6 are the contributions of $\lambda_{i11}\lambda_{i32}^*$ and $\lambda_{i11}^*\lambda_{i23}$, respectively. It is interesting to note that the t -channel RPV sneutrino exchange could enhance $\mathcal{B}(B_s \rightarrow e^+e^-)$ by about 6 orders of magnitude [Figs. 5(b) and 6(b)]. Moreover, they could give distinguishable contributions to $d\mathcal{B}(B \rightarrow Ke^+e^-)/d\hat{s}$ in the high \hat{s} region. For other observables, their contributions are indistinguishable from hadronic uncertainties.

The RPV squark exchange contributions to $B \rightarrow K^{(*)}\mu^+\mu^-$ and $B_s \rightarrow \mu^+\mu^-$ are presented in Fig. 7. Such contributions could give large $\mathcal{A}_{\text{FB}}(B \rightarrow K^*\mu^+\mu^-)$ in favor of Belle and BABAR measurements, however, small corrections to $\mathcal{B}(B_s \rightarrow \mu^+\mu^-)$.

The RPV sneutrino exchange contributions to $B \rightarrow K^*\mu^+\mu^-$ and $B_s \rightarrow \mu^+\mu^-$ are displayed in Figs. 8 and 9, respectively. From plots in these two figures, we find $\mathcal{B}(B_s \rightarrow \mu^+\mu^-)$ is very sensitive to such contributions. Within the constrained parameter space for $\lambda_{i22}\lambda_{i32}^*$ and $\lambda_{i22}^*\lambda_{i23}$, RPV contributions can enhance $\mathcal{B}(B_s \rightarrow \mu^+\mu^-)$ by two orders, which could be accessible at LHC and Tevatron in the forthcoming years. We also note that these

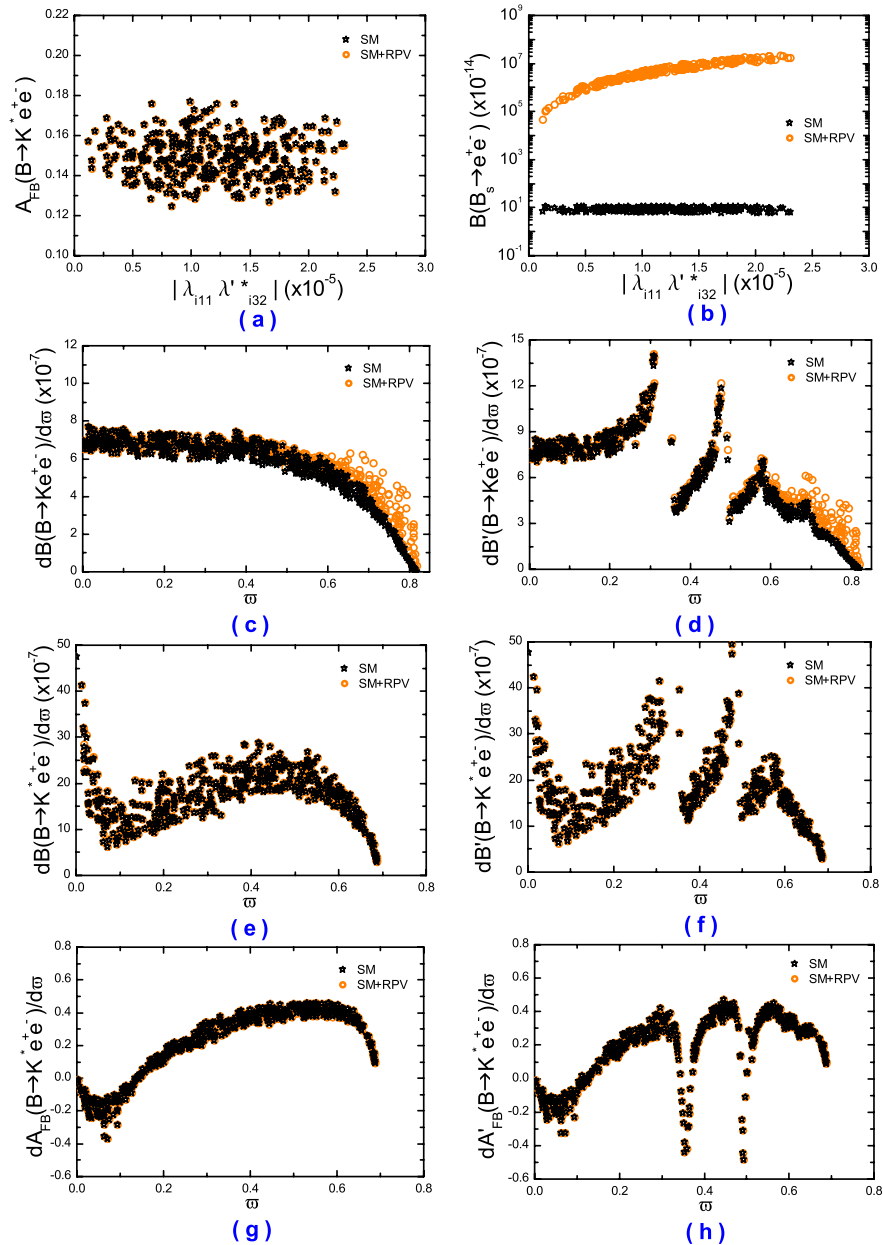


FIG. 5 (color online). The effects of RPV coupling $\lambda_{i11}\lambda_{i32}^*$ due to the sneutrino exchange in $B \rightarrow K^{(*)}e^+e^-$ and $B_s \rightarrow e^+e^-$ decays.

contributions to other observables are small, regarding the large theoretical uncertainties.

It is worth to note that, in the $BABAR$ measurement [1], the value of $\mathcal{A}_{\text{FB}}(B \rightarrow K^* \ell^+ \ell^-)$ with 95% C. L. lower limit is slightly above the SM prediction in the low \hat{s} region. We have found that the RPV couplings $\lambda'_{1i3} \lambda_{1i2}^*$ and $\lambda'_{2i3} \lambda_{2i2}^*$ could enhance $\mathcal{A}_{\text{FB}}(B \rightarrow K^* \ell^+ \ell^-)$ to accommodate the possible discrepancy, which are shown by the following Figs. 4(g) and 7(g), respectively.

Generally, the predictions of B decays suffer from many theoretical uncertainties. Recently, beyond naive factorization, $B \rightarrow K^*$ have been investigated with the QCD factorization [31] framework in [32,33], and then studied with soft collinear effective theory (SCET) [34] in Ref. [35].

However, the power corrections are found to be associated with large theoretical uncertainties, and we are conservative to the naive factorization in this paper.

To probe new physics effects, it would be very useful to measure correlative observables, for example, $d\mathcal{A}_{\text{FB}}(B \rightarrow K^* \mu^+ \mu^-)/d\hat{s}$, $d\mathcal{B}(B \rightarrow K^* \mu^+ \mu^-)/d\hat{s}$, and $\mathcal{B}(B_s \rightarrow \mu^+ \mu^-)$, since correlations among these observables could provide very strict bound on new physics models. At the present, one may have to wait for the error bars in the measurements of these observables to come down and more channels to be measured. With the operation of B factory experiments, large amounts of experimental data on hadronic B meson decays are being collected, and measurements of a previously

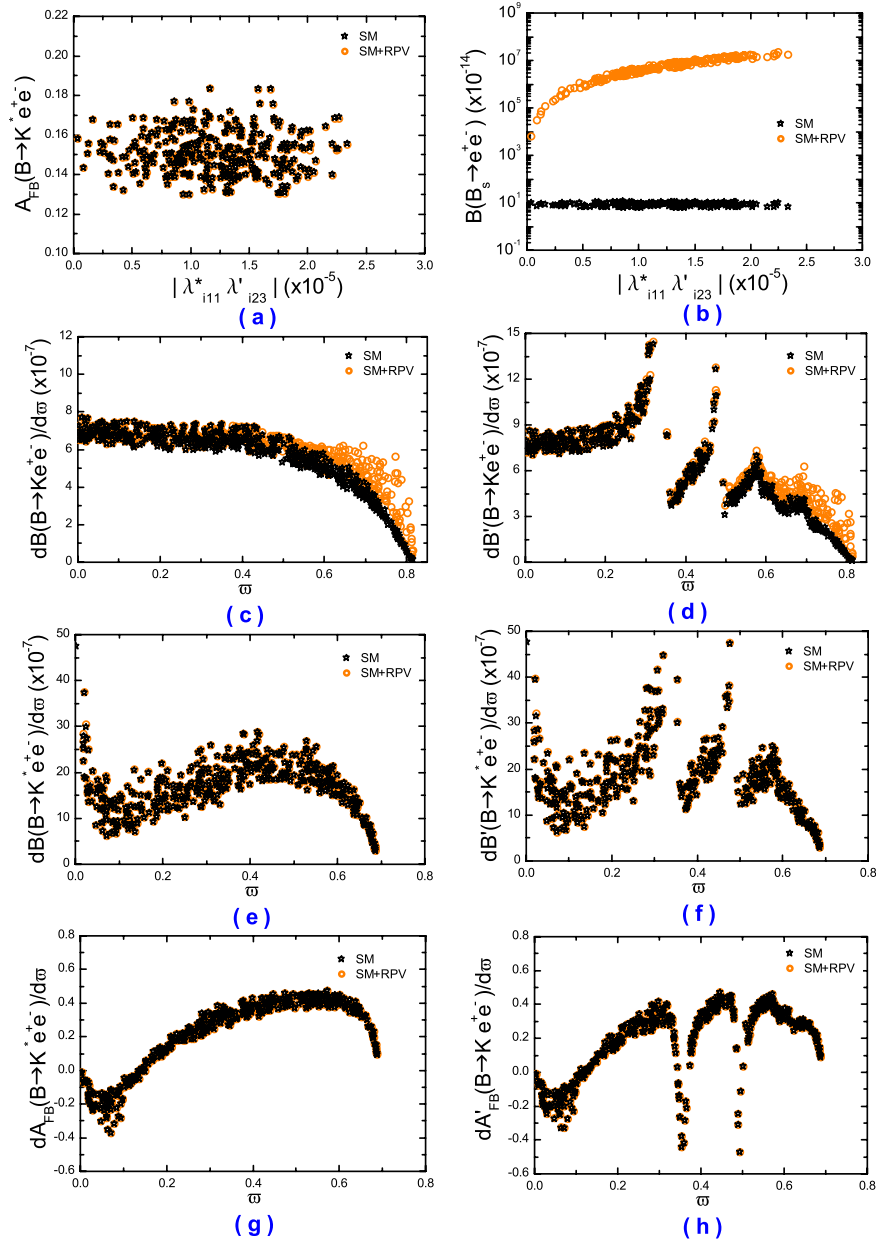


FIG. 6 (color online). The effects of RPV coupling $\lambda'_{i11} \lambda'_{i23}$ due to the sneutrino exchange in $B \rightarrow K^{(*)} e^+ e^-$ and $B_s \rightarrow e^+ e^-$ decays.

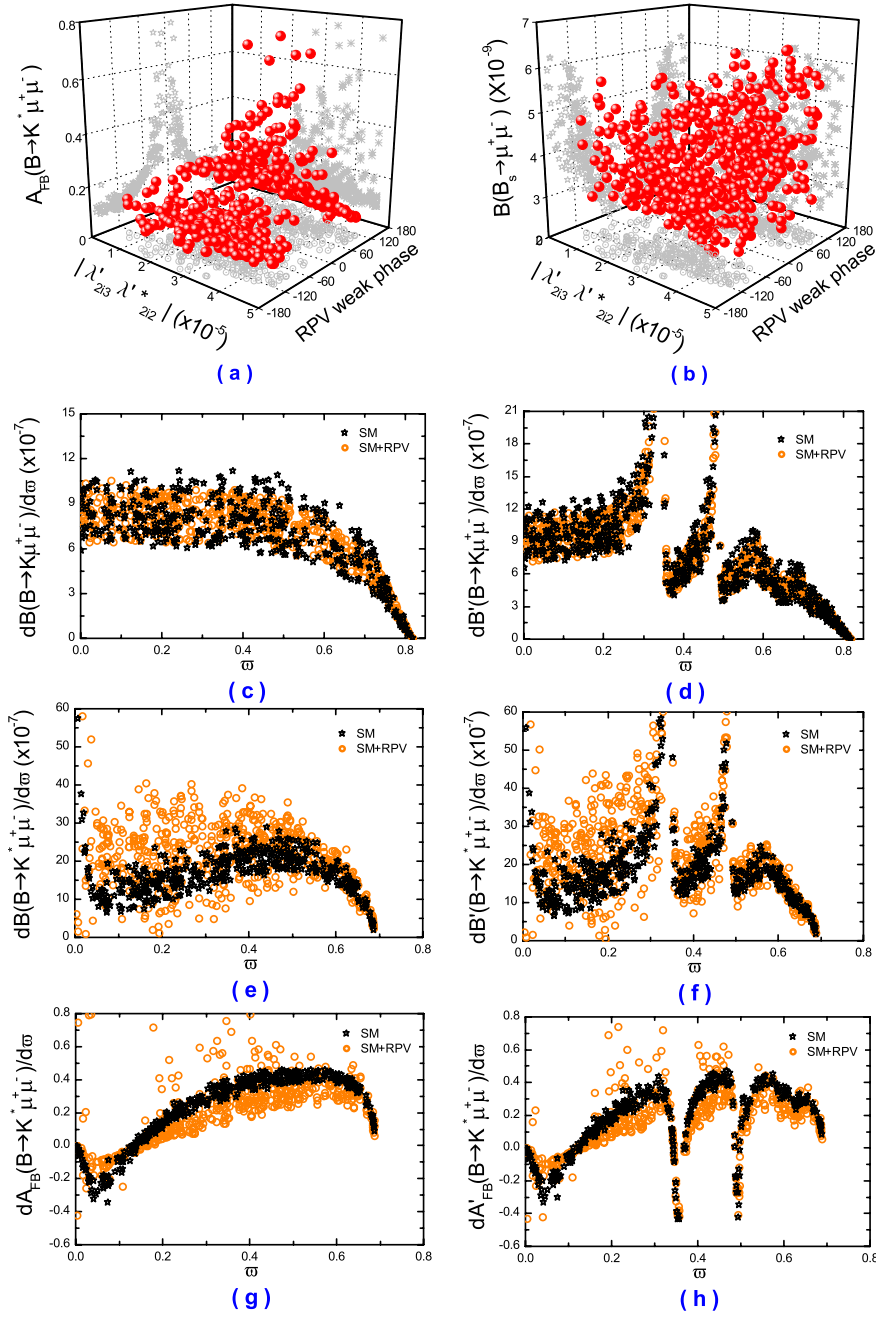


FIG. 7 (color online). The effects of RPV coupling $\lambda'_{213}\lambda_{212}^*$ due to the squark exchange in $B \rightarrow K^{(*)}\mu^+\mu^-$ and $B_s \rightarrow \mu^+\mu^-$ decays.

known observable will become more precise. From the comparison of our predictions in Figs. 4–9 with the near future experiments, one will obtain more stringent bounds on the products of RPV couplings. On the other hand, the RPV SUSY predictions of other decays will become more precise by the more stringent bounds on the RPV couplings.

IV. CONCLUSIONS

In conclusion, the decays $B \rightarrow K^{(*)}\ell^+\ell^-$ and $B_s \rightarrow \ell^+\ell^-$ are very promising means to probe effects of new

physics scenarios. In this paper, we have studied the $B \rightarrow K^{(*)}\ell^+\ell^-$ and $B_s \rightarrow \ell^+\ell^-$ decays in the RPV SUSY model. We have obtained fairly constrained parameter spaces of the RPV coupling products from the present experimental data of $\mathcal{B}(B \rightarrow K^{(*)}\ell^+\ell^-)$ and upper limits of $\mathcal{B}(B_s \rightarrow \ell^+\ell^-)$, and found these constraints are stronger than the existing ones, which may be useful for further studies of the RPV SUSY phenomenology. Furthermore, using the constrained parameter spaces, we have presented the RPV effects on the forward-backward asymmetries of $B \rightarrow K^{(*)}\ell^+\ell^-$ and the branching ratios of the pure lep-

tonic B_s decays. Our results of $\mathcal{A}_{\text{FB}}(B \rightarrow K^{(*)}\ell^+\ell^-)$ agree with the recent experimental data. It is shown that $\mathcal{B}(B_s \rightarrow \ell^+\ell^-)$ could be enhanced several orders by the RPV couplings from the sneutrino exchange. Since we have poorly experimental information about the pure leptonic decay $B_s \rightarrow \ell^+\ell^-$, a further refined upper bound for $\mathcal{B}(B_s \rightarrow \ell^+\ell^-)$ can further restrict the constrained space of the four RPV couplings from the sneutrino exchange. We have also compared the SM predictions with the RPV

predictions about dilepton invariant mass spectra and the normalized forward-backward asymmetries in $B \rightarrow K^{(*)}\ell^+\ell^-$ decays. We have found that $d\mathcal{B}(B \rightarrow K\ell^+\ell^-)/d\hat{s}$ could be mildly decreased by the RPV coupling $\lambda'_{13}\lambda_{12}^{f*}$, and the $\lambda'_{213}\lambda_{212}^{f*}$ contributions to $d\mathcal{B}(B \rightarrow K\mu^+\mu^-)/d\hat{s}$ are indistinguishable from the hadronic uncertainties. The other four RPV couplings due to the sneutrino exchange have distinguishable effects on $d\mathcal{B}(B \rightarrow K\ell^+\ell^-)/d\hat{s}$ at high \hat{s} . For the $B \rightarrow K^*\ell^+\ell^-$

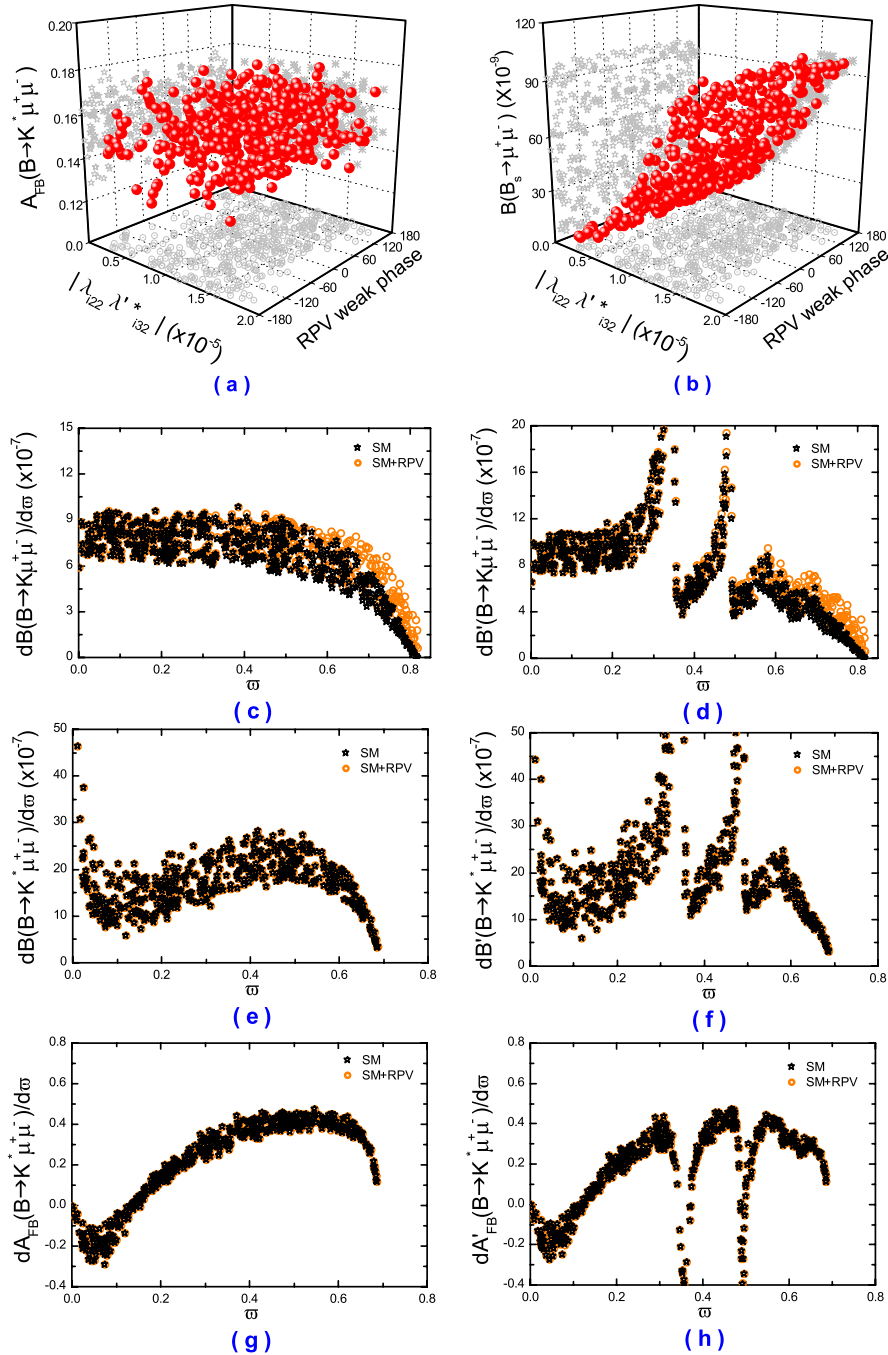


FIG. 8 (color online). The effects of RPV coupling $\lambda_{122}\lambda_{132}^{f*}$ due to the sneutrino exchange in $B \rightarrow K^{(*)}\mu^+\mu^-$ and $B_s \rightarrow \mu^+\mu^-$ decays.

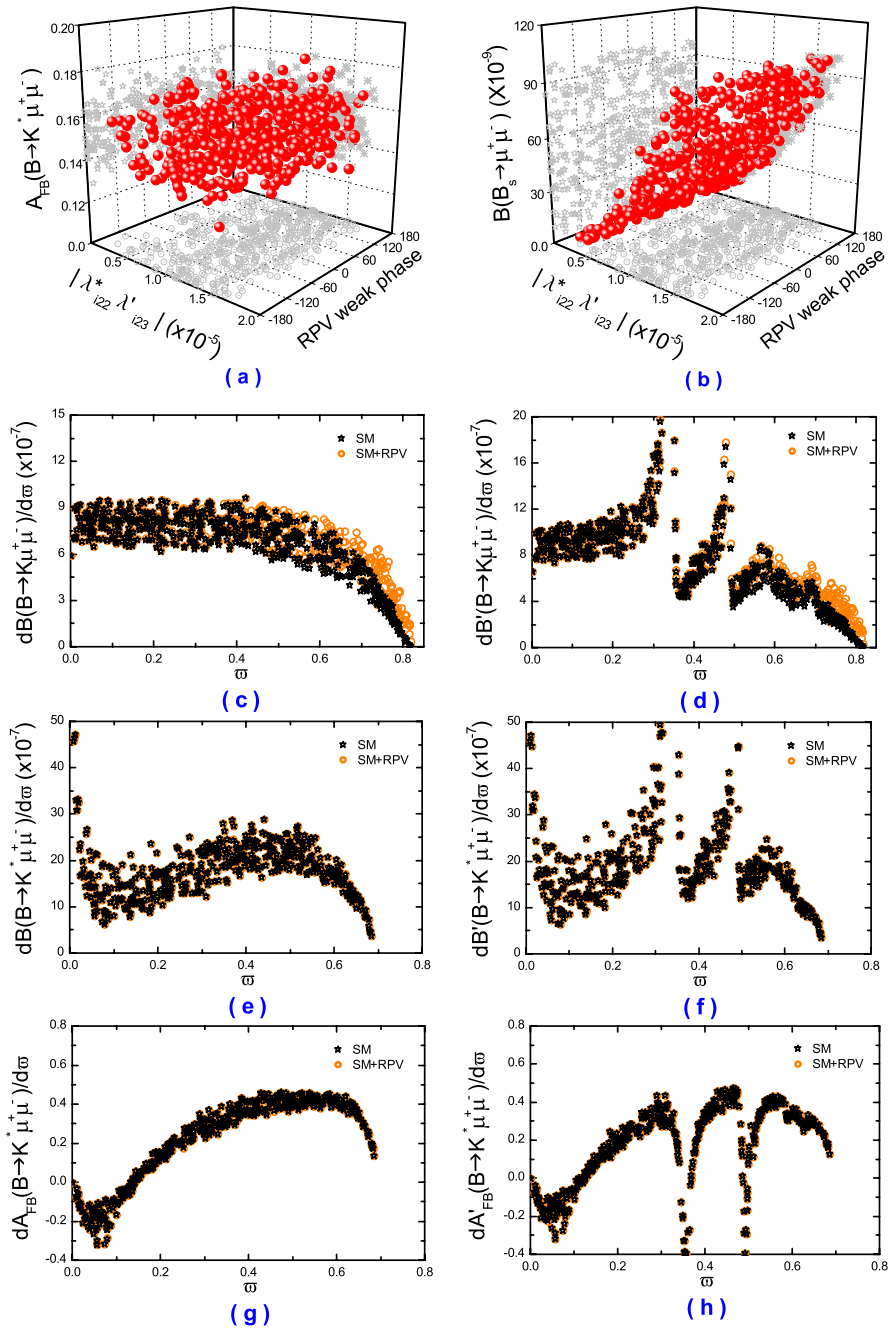


FIG. 9 (color online). The effects of RPV coupling $\lambda_{122}^* \lambda'_{123}$ due to the sneutrino exchange in $B \rightarrow K^{(*)} \mu^+ \mu^-$ and $B_s \rightarrow \mu^+ \mu^-$ decays.

decays, the squark exchange contributions have distinguishable effects on $d\mathcal{B}/d\hat{s}$ and $d\mathcal{A}_{\text{FB}}/d\hat{s}$, but the contributions from the sneutrino exchange have no apparent effects on them. The results in this paper could be useful for probing RPV SUSY effects and will correlate strongly with searches for direct RPV signals at LHC in the forthcoming year.

ACKNOWLEDGMENTS

The work is supported by the National Science Foundation under contracts No. 10305003 and No. 10675039, and the NCET Program sponsored by the Ministry of Education, China, under No. NCET-04-0656.

- [1] B. Aubert *et al.* (BABAR Collaboration), Phys. Rev. D **73**, 092001 (2006).
- [2] K. Abe *et al.* (Belle Collaboration), hep-ex/0410006.
- [3] A. Ishikawa *et al.* (Belle Collaboration), Phys. Rev. Lett. **96**, 251801 (2006).
- [4] Heavy Flavor Averaging Group, <http://www.slac.stanford.edu/xorg/hfag>.
- [5] B. Grinstein, M. J. Savage, and M. B. Wise, Nucl. Phys. **B319**, 271 (1989).
- [6] G. Buchalla and A. J. Buras, Nucl. Phys. **B400**, 225 (1993); M. Misiak, Nucl. Phys. **B393**, 23 (1993); **B439**, 461(E) (1995).
- [7] A. J. Buras and M. Münz, Phys. Rev. D **52**, 186 (1995).
- [8] G. Buchalla, A. J. Buras, and M. E. Lautenbacher, Rev. Mod. Phys. **68**, 1125 (1996).
- [9] A. F. Falk, M. Luke, and M. J. Savage, Phys. Rev. D **49**, 3367 (1994).
- [10] A. Ali, G. Hiller, L. T. Handoko, and T. Morozumi, Phys. Rev. D **55**, 4105 (1997); A. Ali and G. Hiller, Phys. Rev. D **58**, 071501 (1998); **58**, 074001 (1998).
- [11] G. Buchalla and G. Isidori, Nucl. Phys. **B525**, 333 (1998).
- [12] N. G. Deshpande, J. Trampetic, and K. Panose, Phys. Rev. D **39**, 1461 (1989); C. S. Lim, T. Morozumi, and A. I. Sanda, Phys. Lett. B **218**, 343 (1989); A. I. Vainshtein *et al.*, Sov. J. Nucl. Phys. **24**, 427 (1976); P. J. O' Donnell and H. K. K. Tung, Phys. Rev. D **43**, R2067 (1991).
- [13] F. Krüger and L. M. Sehgal, Phys. Lett. B **380**, 199 (1996); M. R. Ahmady, Phys. Rev. D **53**, 2843 (1996); C. D. Lü and Da-Xin Zhang, Phys. Lett. B **397**, 279 (1997).
- [14] A. Ali, T. Mannel, and T. Morozumi, Phys. Lett. B **273**, 505 (1991).
- [15] G. Buchalla, G. Isidori, and S. J. Rey, Nucl. Phys. **B511**, 594 (1998).
- [16] Yuan-Ben Dai, Chao-Shang Huang, and Han-Wen Huang, Phys. Lett. B **390**, 257 (1997); **513**, 429(E) (2001); C. Bobeth *et al.*, Phys. Rev. D **64**, 074014 (2001); G. Erkol and G. Turan, Nucl. Phys. **B635**, 286 (2002); S. Schilling *et al.*, Phys. Lett. B **616**, 93 (2005).
- [17] E. Lunghi *et al.*, Nucl. Phys. **B568**, 120 (2000); D. A. Demir, K. A. Olive, and M. B. Voloshin, Phys. Rev. D **66**, 034015 (2002); Chao-Shang Huang and Xiao-Hong Wu, Nucl. Phys. **B657**, 304 (2003); S. R. Choudhury, A. S. Cornell, N. Gaur, and G. C. Joshi, Phys. Rev. D **69**, 054018 (2004).
- [18] A. Ali, P. Ball, L. T. Handoko, and G. Hiller, Phys. Rev. D **61**, 074024 (2000).
- [19] Wen-Jun Li, Yuan-Ben Dai, and Chao-Shang Huang, Eur. Phys. J. C **40**, 565 (2005).
- [20] Zhen-jun Xiao and Lin-xia Lu, Phys. Rev. D **74**, 034016 (2006).
- [21] G. Bhattacharyya and A. Raychaudhuri, Phys. Rev. D **57**, R3837 (1998); D. Guetta, Phys. Rev. D **58**, 116008 (1998); G. Bhattacharyya and A. Datta, Phys. Rev. Lett. **83**, 2300 (1999); G. Bhattacharyya, A. Datta, and A. Kundu, Phys. Lett. B **514**, 47 (2001); D. Chakraverty and D. Choudhury, Phys. Rev. D **63**, 075009 (2001); **63**, 112002 (2001); D. Choudhury, B. Dutta, and A. Kundu, Phys. Lett. B **456**, 185 (1999); G. Bhattacharyya, A. Datta, and A. Kundu, J. Phys. G **30**, 1947 (2004); B. Dutta, C. S. Kim, and S. Oh, Phys. Rev. Lett. **90**, 011801 (2003); A. Datta, Phys. Rev. D **66**, 071702 (2002); C. Dariescu, M. A. Dariescu, N. G. Deshpande, and D. K. Ghosh, Phys. Rev. D **69**, 112003 (2004); S. Bar-Shalom, G. Eilam, and Y. D. Yang, Phys. Rev. D **67**, 014007 (2003); Ya-Dong Yang, Rumin Wang, and G. R. Lu, Phys. Rev. D **72**, 015009 (2005); **73**, 015003 (2006); R. M. Wang, G. R. Lu, E.-K. Wang, and Y.-D. Yang, Eur. Phys. J. C **47**, 815 (2006).
- [22] J. P. Saha and A. Kundu, Phys. Rev. D **66**, 054021 (2002).
- [23] P. Ball and R. Zwicky, Phys. Rev. D **71**, 014015 (2005); **71**, 014029 (2005).
- [24] G. Buchalla and A. J. Buras, Nucl. Phys. **B400**, 225 (1993).
- [25] S. Weinberg, Phys. Rev. D **26**, 287 (1982).
- [26] R. Barbier *et al.*, Phys. Rep. **420**, 1 (2005).
- [27] W. M. Yao *et al.*, J. Phys. G **33**, 1 (2006).
- [28] S. Hashimoto, Int. J. Mod. Phys. A **20**, 5133 (2005).
- [29] D. Tonelli (CDF Collaboration), eConf C060409, 001 (2006), hep-ex/0605038.
- [30] B. C. Allanach, A. Dedes, and H. K. Dreiner, Phys. Rev. D **69**, 115002 (2004).
- [31] M. Beneke, G. Buchalla, M. Neubert, and C. T. Sachrajda, Phys. Rev. Lett. **83**, 1914 (1999); Nucl. Phys. **B591**, 313 (2000).
- [32] M. Beneke, Th. Feldmann, and D. Seidel, Nucl. Phys. **B612**, 25 (2001).
- [33] M. Beneke and Th. Feldmann, Eur. Phys. J. C **41**, 173 (2005).
- [34] C. W. Bauer, S. Fleming, and M. Luke, Phys. Rev. D **63**, 014006 (2000); C. W. Bauer, S. Fleming, D. Pirjol, and I. W. Stewart, Phys. Rev. D **63**, 114020 (2001); C. W. Bauer and I. W. Stewart, Phys. Lett. B **516**, 134 (2001); C. W. Bauer, D. Pirjol, and I. W. Stewart, Phys. Rev. D **65**, 054022 (2002).
- [35] A. Ali, G. Kramer, and G. H. Zhu, Eur. Phys. J. C **47**, 625 (2006); A. Ali, hep-ph/0609114.